ON-ROAD AND CHASSIS DYNAMOMETER TESTING OF LIGHT-DUTY DIESEL PASSENGER CARS

Marc C. Besch, Sri Hari Chalagalla, and Dan Carder
Center for Alternative Fuels, Engines, and Emissions
West Virginia University

EXECUTIVE SUMMARY

Tests were conducted on 5 model year (MY) 2014 and 2015 vehicles produced by Fiat Chrysler Automobiles (FCA). The test vehicles comprised Jeep Grand Cherokees and Ram 1500 diesel vehicles, all equipped with the 3.0L EcoDiesel engine, and featuring selective catalytic reduction (SCR) NO_x after-treatment technology. All test vehicles were evaluated on a vehicle chassis dynamometer as well as over-the-road, during a variety of driving conditions including urban/suburban and highway driving. In addition, one of the Jeep Grand Cherokee and one of the Ram 1500 vehicles was tested prior to, as well as after a mandatory vehicle recall conducted by the manufacturer (i.e. FCA) that concerned the emissions control systems.

For both types of testing, gaseous exhaust emissions, including oxides of nitrogen (NO_x), nitrogen oxide (NO), carbon monoxide (CO), carbon dioxide (CO_2), and total hydrocarbons (THC) were measured on a continuous basis utilizing a portable emissions measurement system (PEMS) from Horiba®. Additionally, total particle number concentrations were quantified using a real-time particle sensor from Pegasor (PPS). The primary objective of the study was to characterize the performance of NO_x after-treatment conversion efficiencies of the vehicles when they are being tested in the laboratory (i.e. chassis dynamometer) as well as over-the-road (i.e. on-road) to elucidate the impact of driving conditions, ambient conditions and exhaust gas thermodynamic properties.

Results indicated that both Jeep Grand Cherokee and Ram 1500 in MY 2014 exhibited, in general, significantly increased NO_x emissions during on-road operation as compared to the chassis dynamometer results. For MY 2015, Jeep vehicles produced from 4 to 8 times more NO_x emissions during urban/rural on-road operation than the certification standard, while Ram 1500

vehicles had maximum NO_x emission deviation factors of approximately 25 times above the US-EPA Tier2-Bin5 standard, for highway driving conditions.

TABLE OF CONTENTS

LIST OF TABLES

LIST OF FIGURES

LIST OF ABBREVIATIONS AND UNITS

CAFEE	-	Center for Alternative Fuels, Engines and Emissions
CARB	-	California Air Resources Board
CLD	-	Chemiluminescence Detector
CO	-	Carbon Monoxide
CO_2	-	Carbon Dioxide
CVS	-	Constant Volume Sampler
DPF	-	Diesel Particle Filter
EERL	-	Engines and Emissions Research Laboratory
EFM	-	Exhaust Flow Meter
EPA	-	Environmental Protection Agency
EU	-	European Union
FTP	-	Federal Test Procedure
GPS	-	Global Positioning System
FCA	-	Fiat Chrysler Automobiles
FID	-	Flame Ionization Detector
LNT	-	Lean NO_x Trap
MPG	-	Miles per Gallon
NDIR	-	Non-Dispersive Infrared Spectrometer
NEDC	-	New European Driving Cycle
NO	-	Nitrogen Monoxide
NO_x	-	Oxides of Nitrogen
NTE	-	Not-to-Exceed
OC	-	Oxidation Catalyst
PEMS	-	Portable Emissions Measurement System
PM	-	Particulate Matter
PN	-	Particle Number
RPA	-	Relative Positive Acceleration
SCR	-	Selective Catalytic Reduction
THC	-	Total Hydrocarbons

1 INTRODUCTION

The primary objective of the study was to characterize real-world emissions of NO_x and other regulated gaseous pollutants as well as evaluate the performance of NO_x after-treatment conversion efficiencies of the 6 light-duty vehicles when being tested in the laboratory (i.e. chassis dynamometer) as well as over-the-road (i.e. on-road) and present the data as a function of driving conditions, traffic density, ambient conditions and exhaust gas thermodynamic properties. All test vehicles were equipped with diesel engines and selective catalytic reduction (SCR) technology based after-treatment systems, and were certified to US-EPA Tier2-Bin5 and CARB LEV-II (CA) standards. Emissions were measured during vehicle chassis dynamometer testing over standardized test cycles used for vehicle certification as prescribed by the code of federal regulations (CFR), and during on-road operation characterized by a mix of urban and highway driving conditions using a portable emissions measurement system (PEMS).

Gaseous exhaust emissions, including oxides of nitrogen (NO_x), nitrogen oxide (NO), carbon monoxide (CO), and carbon dioxide (CO_2) were measured on a continuous basis utilizing a Horiba® OBS-ONE PEMS instrument, whereas particle number concentrations and particulate mass emissions were inferred from real-time measurements performed using a Pegasor particle sensor, model PPS-M from Pegasor Ltd.

For years, the use of standardized test cycles has received much criticism over their representativeness of real-world operation. As such, on-road test routes were translated into dynamometer test cycles so that the test vehicles could be operated against similar speed and load requirements in a controlled laboratory setting. It is noted that for these cycles, engine loading required to overcome road-grade was not included as part of the simulation. Therefore, total energy expended would be lower for the simulated cycles when compared to the actual on-road routes, with an increased difference for routes that included operation over increased elevation changes.

Specifically, the data collected during the course of this study allowed for following analysis and comparisons:

i. comparison of off-cycle NO_x emissions against US-EPA Tier 2-Bin 5 and CARB LEV-II ULEV emissions standards;

ii. comparison of NO_x emissions between on-road routes and chassis dynamometer cycles developed from route vehicle speed profiles;

iii. evaluation of emissions conversion efficiencies prior and after a mandatory vehicle recall by the manufacturer that concerned the emissions control systems;

iv. evaluation of fuel economy in comparison to standardized chassis dynamometer test cycles and EPA evaluated fuel economy ratings as published on window stickers for new cars sold in the United States [1];

v. evaluation of SCR NO_x after-treatment conversion efficiencies as a function of driving conditions, traffic density, ambient conditions (e.g. ambient temperature) and exhaust gas thermodynamic properties;

vi. quantification of particle number (PN) emissions concentrations with regards to the particle number limits (i.e. $6.0x10^{11}$ #/km) set forth by the European Union (EU) in 2013 with the introduction of Euro 5b/b+ emission standards [3].

2 REVIEW OF REGULATORY REQUIREMENT FOR TIER 2 / LEV-II

Emissions of light-duty vehicles are currently regulated under EPA's Tier 2 and California LEV-II emissions regulations. EPA's vehicle classification is based on gross vehicle weight rating (GVWR) and is shown in Table 2.1. It should be noted that medium duty passenger vehicles (MDPV) are also regulated under light-duty vehicle emissions regulations.

Table 2.1: Vehicle classification based on gross vehicle weight rating (GVWR) [4].

	Gross Vehicle Weight Rating (GVWR) [lbs]									
	6,000	8,500	10,500	14,000	16,000	19,500	26,000	33,000	60,000	
Federal	LDV		MDPV[c]							
	LDT		HDV / HDE							
	LLDT	HLDT	LHDDE				MHDDE		HHDDE / Urban Bus	
	LDT 1 & 2[a]	LDT 3 & 4[b]	HDV2b	HDV3	HDV4	HDV5	HDV6	HDV7	HDV8a	HDV8b

[a] *Light-duty truck (LDT) 1 if loaded vehicle weight (LVW) = 3,750; LDT 2 if LVW > 3,750*

[b] *LDT 3 if adjusted loaded vehicle weight (ALVW) = 5,750; LDT 4 if ALVW > 5,750*

[c] *MDPV vehicles will generally be grouped with and treated as HLDTs in the Tier 2 program*

The EPA's Tier 2 emission standards that were phased in over a period of four years, beginning in 2004, for LDV/LLDTs, with an extension of two years for HLDTs, were in full effect starting from MY 2009 for all new passenger cars and light-duty trucks, including pickup trucks, vans, minivans and sport-utility vehicles. The Tier 2 standards were designed to significantly reduce ozone-forming pollution and PM emissions from passenger vehicles regardless of the fuel used and the type of vehicle, namely car, light-duty truck or larger passenger vehicle. The Tier 2 standards were implemented along with the gasoline fuel sulfur standards in order to enable emissions reduction technologies necessary to meet the stringent vehicle emissions standards. The gasoline fuel sulfur standard mandates the refiners and importers to meet a corporate average gasoline sulfur standard of 30 ppm starting from 2006 [5].

The EPA Tier 2 emissions standard requires each LDV/LDT vehicle manufacturer to meet a corporate average NO_x standard of 0.07g/mile (0.04 g/km) for the fleet of vehicles being sold for a given model year. Furthermore, the Tier 2 emissions standard consists of eight sub-bins, each one with a set of standards to which the manufacturer can certify their vehicles provided the corporate sales weighted average NO_x level over the full useful life of the vehicle (10

years/120,000 miles/193,121 km), for a given MY of Tier 2 vehicles, is less than 0.07g/mile (0.04 g/km). The corporate average emission standards are designed to meet the air quality goals allowing manufacturers the flexibility to certify some models above or below the standard, thereby enabling the use of available emissions reduction technologies in a cost-effective manner as opposed to meeting a single set of standards for all vehicles [5]. Final phased-in full and intermediate useful life Tier 2 standards are listed in Table 2.2.

Table 2.2: Light-duty vehicle, light-duty truck, and medium-duty passenger vehicle - EPA Tier 2 exhaust emissions standards in [g/miles] [5].

Bin#	Intermediate life (5 years / 50,000 mi)					Full useful life (10 years/120,000 mi)				
	NMOG*	CO	NO_x	PM	HCHO	NMOG*	CO	NO_x†	PM	HCHO
Temporary Bins										
11 MDPV[c]						0.28	7.3	0.90	0.12	0.032
10[a,b,d,f]	0.125 (0.160)	3.4 (4.4)	0.40	-	0.015 (0.018)	0.156 (0.230)	4.2 (6.4)	0.60	0.08	0.018 (0.027)
9[a,b,e,f]	0.075 (0.140)	3.4	0.20	-	0.015	0.090 (0.180)	4.2	0.30	0.06	0.018
Permanent Bins										
8[b]	0.100 (0.125)	3.4	0.14	-	0.015	0.125 (0.156)	4.2	0.20	0.02	0.018
7	0.075	3.4	0.11	-	0.015	0.09	4.2	0.15	0.02	0.018
6	0.075	3.4	0.08	-	0.015	0.09	4.2	0.10	0.01	0.018
5	0.075	3.4	0.05	-	0.015	0.09	4.2	0.07	0.01	0.018
4	-	-	-	-	-	0.07	2.1	0.04	0.01	0.011
3	-	-	-	-	-	0.055	2.1	0.03	0.01	0.011
2	-	-	-	-	-	0.01	2.1	0.02	0.01	0.004
1	-	-	-	-	-	0	0	0	0	0

** for diesel fueled vehicle, NMOG (non-methane organic gases) means NMHC (non-methane hydrocarbons)*
† average manufacturer fleet NO_x standard is 0.07 g/mi for Tier 2 vehicles
a *Bin deleted at end of 2006 model year (2008 for HLDTs)*
b *The higher temporary NMOG, CO and HCHO values apply only to HLDTs and MDPVs and expire after 2008*
c *An additional temporary bin restricted to MDPVs, expires after model year 2008*
d *Optional temporary NMOG standard of 0.195 g/mi (50,000) and 0.280 g/mi (full useful life) applies for qualifying LDT4s and MDPVs only*
e *Optional temporary NMOG standard of 0.100 g/mi (50,000) and 0.130 g/mi (full useful life) applies for qualifying LDT2s only*
f *50,000 mile standard optional for diesels certified to bins 9 or 10*

All Tier 2 exhaust emissions standards must be met over the FTP-75 chassis dynamometer test cycle. In addition to the above listed emissions standards, Tier 2 vehicles must also satisfy the supplemental FTP (SFTP) standards. The SFTP standards are intended to control emissions from

vehicles when operated at high speed and acceleration rates (i.e. aggressive driving, as simulated through the US06 test cycle), as well as when operated under high ambient temperature conditions with vehicle air-conditioning system turned on (simulated through the SC03 test cycle). The SFTP emissions results are determined using the relationship outlined in Equation 1 where individual emissions measured in [g/mi] over FTP, US06 and SC03 test cycles are added together with different weighting factors. The thereby calculated emissions are then compared to the SFTP standard to evaluate compliance at 4000 miles and full useful file (i.e. 120,000 miles).

$$E_{pollutant} = 0.35 * (FTP) + 0.28 * (US06) + 0.37 * (SC03) \quad \textbf{Eq. 1}$$

Manufacturers must comply with 4000 mile and full useful life SFTP standards. The 4000 mile SFTP standards are shown in Table 2.3.

Table 2.3: US-EPA 4000 mile SFTP standards in [g/mi] for Tier 2 vehicles [5].

Vehicle Class [1)]	US06		SC03	
	NMHC + NO_x	CO	NMHC + NO_x	CO
LDV/LDT1	0.14	8.0	0.20	2.7
LDT2	0.25	10.5	0.27	3.5
LDT3	0.40	10.5	0.31	3.5
LDT4	0.60	11.8	0.44	4.0

1) *Supplemental exhaust emission standards are applicable to gasoline and diesel-fueled LDV/LDTs but are not applicable to MDPVs, alternative fueled LDV/LDTs, or flexible fueled LDV/LDTs when operated on a fuel other than gasoline or diesel*

The full useful life SFTP standards are determined following Equation 2, which is based on Tier 1 SFTP standards, lowered by 35% of the difference between the Tier 2 and Tier 1 exhaust emissions standards. Tier 1 full useful life SFTP standards for different vehicle classes along with CO standards for individual chassis dynamometer test cycles as well as Tier 1 full useful life FTP standards are shown in Table 2.4 and Table 2.5, respectively.

$$Tier\ 2\ SFTP_{std} = Tier\ 1\ SFTP_{std} - 0.35 * (Tier\ 1\ FTP_{std} - Tier\ 2\ FTP_{std}) \quad \textbf{Eq. 2}$$

Table 2.6 lists the calculated US-EPA Tier 2 full useful live SFTP standards in [g/mi] for different vehicle weight classes for Tier 2 emissions Bins 4 through 5.

Table 2.4: US-EPA Tier 1 full useful life SFTP standards in [g/mi] [5].

Vehicle Class	NMHC + NO_x [a,c]	CO [b,c]		
		US06	SC03	Weighted
LDV/LDT1	0.91 (0.65)	11.1 (9.0)	3.7 (3.0)	4.2 (3.4)
LDT2	1.37 (1.02)	14.6 (11.6)	4.9 (3.9)	5.5 (4.4)
LDT3	1.44	16.9	5.6	6.4
LDT4	2.09	19.3	6.4	7.3

a) *Weighting for NMHC + NO_x and optional weighting for CO is 0.35*(FTP) + 0.28*(US06) + 0.37*(SC03)*

b) *CO standards are stand alone for US06 and SC03 with option for a weighted standard*

c) *Intermediate life standards are shown in parentheses for diesel LDV/LLDTs opting to calculate intermediate life SFTP standards in lieu of 4,000 mile SFTP standards as permitted.*

Table 2.5: US-EPA Tier 1 full useful life FTP standards in [g/mi] [5].

Vehicle Class	NMHC [a]	NO_x [a]	CO [a]	PM
LDV/LDT1	0.31 (0.25)	0.60 (0.40)	4.2 (3.4)	0.10
LDT2	0.40 (0.32)	0.97 (0.70)	5.5 (4.4)	0.10
LDT3	0.46	0.98	6.4	0.10
LDT4	0.56	1.53	7.3	0.12

a) *Intermediate life standards are shown in parentheses for diesel LDV/LLDTs opting to calculate intermediate life SFTP standards in lieu of 4,000 mile SFTP standards as permitted*

Table 2.6: US-EPA Tier 2 full useful life SFTP standards in [g/mi] for Bin 4 through Bin 6.

Vehicle Class	Bin 4	Bin 5	Bin 6
LDV/LDT1	0.63	0.65	0.66
LDT2	0.93	0.95	0.96
LDT3	0.97	0.99	1.00
LDT4	1.40	1.41	1.43

In-use testing of light duty vehicles under the Tier 2 regulation involves testing of vehicles on a chassis dynamometer that have accumulated at least 50,000 miles during in-use operation, to verify compliance with FTP and SFTP emissions standards at intermediate useful life. There has been no regulatory requirement in the United States to verify compliance of Tier 2 vehicles for emissions standards over off-cycle tests such as on road emissions testing with the use of PEMS equipment, similar to what is being mandated for heavy-duty vehicles via the engine in-use compliance requirements (i.e. NTE emissions). Meanwhile, the European Commission (EC) has established a working group to propose modifications to its current vehicle certification procedures in order to better limit and control off-cycle emissions [6]. Over the course of a two-year evaluation process, different approaches were being assessed with two of them believed to be promising for

application in a future light-duty emissions regulation, namely; i) emissions testing with random driving cycle generation in the laboratory, and ii) on-road emissions testing with PEMS equipment [6].

Fuel economy and CO_2 emission ratings as published by the US-EPA and the US Department of Energy (DOE) are based on laboratory testing of vehicles while being operated over a series of five driving cycles on a chassis dynamometer specified in more detail in Table 2.7 [1].

Table 2.7: Fuel economy and CO_2 emissions test characteristics [1].

Driving Schedule Attributes	Test Schedule				
	City	**Highway**	**High Speed**	**AC**	**Cold Temp.**
Trip type	Low speeds in stop-and-go urban traffic	Free-flow traffic at highway speeds	Higher speeds; harder accel. and braking	AC use under hot ambient conditions	City test w/ colder outside temperature
Max. speed [mph]	56	60	80	54.8	56
Avg. speed [mph]	21.2	48.3	48.4	21.2	21.2
Max. accl. [mph/s]	3.3	3.2	8.46	5.1	3.3
Distance [miles]	11	10.3	8	3.6	11
Duration [min]	31.2	12.75	9.9	9.9	31.2
Stops [#]	23	None	4	5	23
Idling time [%] [1)]	18	None	7	19	18
Engine Startup [2)]	Cold	Warm	Warm	Warm	Cold
Lab temperature [°F]	68 - 86	68 - 86	68 - 86	95	20
Vehicle AC	Off	Off	Off	On	Off

[1)] *Idling time in percent of total test duration*

[2)] *Maximum fuel efficiency is not reached until engine is in warmed up condition*

Originally, only the '*city*' (i.e. FTP-75) and '*highway*' cycles were used to determine vehicle fuel economy, however, starting with model year 2008 vehicles the test procedure has been augmented by three additional driving schedules, specifically, '*high-speed*' (i.e. US06), '*air conditioning*' (i.e. SC03 with air conditioning turned on), and '*cold temperature*' (i.e. FTP-75 at 20°F ambient temperature) driving cycles [1]. Vehicle manufacturer are required to test a number of vehicles representative of all available combinations of engine, transmission and vehicle weight

classes being sold in the US. The fuel economy label provides distance-specific fuel consumption and CO_2 emissions values for '*city*', and '*highway*' driving as well as a combined value (i.e. Combined MPG) calculated as a weighted average of 55% '*city*' and 45% '*highway*' driving, allowing for a simplified comparison of fuel efficiency across different vehicles [1].

3 METHODOLOGY

The following section of the report will discuss the test vehicles used during this study, describe the vehicle chassis dynamometer test cycles and the specific on-road test routes and their characteristics, as well as present the emissions sampling setup and instrumentation utilized during this work.

3.1 Test Vehicle Selection

The vehicles tested in this study comprise two MY 2014 (i.e. one) and MY 2015 (i.e. one) Jeep Grand Cherokee, three MY 2014 (i.e. two) and MY 2015 (i.e. one) Ram 1500 diesel-fueled light-duty trucks and SUVs. All test vehicles were equipped with turbocharged diesel fueled compression ignition (CI) engines in conjunction with aqueous urea-SCR systems and diesel particulate filters (DPF) for NO_x and PM control, respectively. All test vehicles were compliant with EPA Tier2-Bin5, as well as California LEV-II ULEV emissions standards, as per EPA certification documents. All test vehicles were categorized as '*light-duty truck 4*' (LDT4). Actual CO_2 emissions and fuel economy for city, highway, and combined driving conditions, as advertised by the EPA for new vehicles sold in the US are given in Table 3.1 and Table 3.2 for the respective test vehicles.

All test vehicles were thoroughly checked for possible engine or after-treatment malfunction codes using an ECU scanning tool prior to selecting a vehicle for this on-road measurement campaign, with none of them showing any fault code or other anomalies. More specific details for all test vehicles are presented in Table 3.1 and Table 3.2.

In addition, one Ram 1500 (i.e. *Vehicle 1d*) and one Jeep Grand Cherokee (i.e. *Vehicle 2b*) were subject to a vehicle service recall by the manufacturer in regards to their emissions control system. The particular recall was termed '*Emissions Recall R69 Selective Catalytic Reduction Catalyst*' (http://wk2jeeps.com/, tsb/rc_R6916.pdf). As part of the herein presented study both vehicles (i.e. *Vehicle 1d and 2b*) would be tested prior as well as after the recall was completed by a local FCA service and dealership center.

Table 3.1: Test vehicles and engine specifications for Jeep Grand Cherokee.

Vehicle		**Vehicle 2**	**Vehicle 2b**
Make / Model		Jeep Grand Cherokee	Jeep Grand Cherokee
Model year		2015	2014
Engine family		FCRXT03.05PV	ECRXT03.05PV
VIN		1C4RJFBM0FC179087	1C4RJFCM6EC551125
Recall state (R69)		None	pre- / post-recall
Mileage at test start [miles]		2,571	25,119
Fuel		ULSD (pump fuel)	ULSD (pump fuel)
Engine displacement [L]		3.0	3.0
Engine aspiration		Turbocharged/ Intercooled	Turbocharged/ Intercooled
Max. engine power [kW]		240 @ 3600 rpm	
Max. engine torque [Nm]		569 @ 2000 rpm	
Emission after-treatment technology		OC, DPF, urea-SCR	OC, DPF, urea-SCR
Drive train		4-wheel drive	4-wheel drive
Applicable emissions limit	*U.S. EPA*	T2B5 (LDT4)	T2B5 (LDT4)
	CARB	LEV-II ULEV	LEV-II ULEV
EPA Fuel Economy Values [mpg] [1)]	*City*	21	21
	Highway	28	28
	Combined	24	24
EPA CO_2 Values [g/mile] [1)]		432	432

1) *EPA advertised fuel economy and CO_2 emissions values for new vehicles in the US (www.fueleconomy.gov)*

Table 3.2: Test vehicles and engine specifications for Ram 1500.

Vehicle		**Vehicle 1**	**Vehicle 1c**	**Vehicle 1d**
Make / Model		Ram 1500	Ram 1500	Ram 1500
Model year		2015	2014	2014
Engine family		FCRXT03.05PV	ECRXT03.05PV	ECRXT03.05PV
VIN		1C6RR7GM7FS710936	C6RR7TM7ES376489	1C6RR7FM1ES480164
Recall state (R69)		None	None	pre- / post-recall
Mileage at test start [miles]		1,901	28,924	43,236
Fuel		ULSD (pump fuel)	ULSD (pump fuel)	ULSD (pump fuel)
Engine displacement [L]		3.0	3.0	3.0
Engine aspiration		Turbocharged/ Intercooled	Turbocharged/ Intercooled	Turbocharged/ Intercooled
Max. engine power [kW]			240 @ 3600 rpm	
Max. engine torque [Nm]			569 @ 2000 rpm	
Emission after-treatment technology		OC, DPF, urea-SCR	OC, DPF, urea-SCR	OC, DPF, urea-SCR
Drive train		4-wheel drive	2-wheel drive	2-wheel drive
Applicable emissions limit	*U.S. EPA*	T2B5 (LDT4)	T2B5 (LDT4)	T2B5 (LDT4)
	CARB	LEV-II ULEV	LEV-II ULEV	LEV-II ULEV
EPA Fuel Economy Values [mpg] [1)]	*City*	19	20	20
	Highway	26	27	27
	Combined	22	23	23
EPA CO_2 Values [g/mile] [1)]		461	440	440

1) *EPA advertised fuel economy and CO_2 emissions values for new vehicles in the US (www.fueleconomy.gov)*

Table 3.3 lists the individual curb weights, gross vehicle weight ratings (GVWR), and actual test weights while performing the on-road PEMS testing. Actual test weights were calculated as the sum of manufacturer specified vehicle curb weights and the individual weights of the instrumentation and driver. The payload comprised the entire instrumentation and associated equipment, including pressurized gas bottles for the emissions analyzers, as well as the weight of a driver and passenger of 77kg each. Table 3.3 further allows for a comparison between the actual test weight of the vehicles during PEMS testing and the respective equivalent test weight (ETW) as applied during emissions certification testing on the chassis dynamometer according to 40 CFR paragraph 86.129-00(f)(1).

The diesel fuel used during this study was commercially available ultra-low diesel fuel (ULSD) in Morgantown, WV. Careful attention was paid to procuring the test fuel for both chassis dynamometer and on-road testing from one single fuel station (i.e. Sheetz, Downtown, Morgantown) in order to minimize variability that could possibly originate from use of different diesel fuel brands.

Table 3.3: Test weights for vehicles

Vehicle	Curb Weight [lbs]	GVWR [lbs]	Equiv. Test Weight [lbs]	Actual Test Weight [lbs]	Payload [lbs]
Ram 1500	5792	6950	6000	6592	800
Jeep Cherokee	5411	6800	5500	6211	800

3.2 Vehicle Test Cycles and Routes

Emissions characterization of all vehicles was conducted over a series of six light-duty certification, and three real-world chassis dynamometer test cycles presented in Section 3.2.1. On-road testing was performed over two different test routes discussed in Section 3.2.2.

3.2.1 Vehicle Chassis Dynamometer Test Cycles

Table 3.4 and Table 3.5 provide a comparison of characteristics of the six light-duty chassis dynamometer certification and three real-world cycles, respectively, used during this project.

Table 3.4: Comparison of characteristics of light-duty vehicle certification cycles.

Cycle	FTP-75	SC03	US06	HWFET	NEDC	WLTP
Cycle duration [sec]	1876	596	595	780	1179	1800
Cycle distance [km]	17.8	5.8	12.9	16.5	10.9	23.3
Avg. vehicle speed [km/h]	34.1	34.8	78.0	76.1	33.4	46.5
Max. vehicle speed [km/h]	91.2	88.2	129.2	96.4	120.1	131.3
Avg. RPA [1)] [m/s^2]	0.23	0.20	0.53	0.07	0.14	0.20
Characteristic Power [m^2/s^3]	1.65	-	-	-	1.04	-
Share [%] (*time based*)						
- idling (≤2 km/h)	20.2	20.0	7.6	2.7	25.2	14.0
- low speed (>2≤50 km/h)	58.7	48.5	18.4	4.4	43.2	44.7
- medium speed (>50≤90 km/h)	19.6	31.5	17.9	70.3	24.5	26.6
- high speed (>90 km/h)	1.5	0	56.2	22.6	7.1	14.7

[1)] *RPA - relative positive acceleration*

Table 3.5: Comparison of characteristics of light-duty vehicle real-world cycles.

Cycle	MGW Cycle	LA-4 Cycle	Bruceton Cycle	Ann Arbor Cycle
Cycle duration [sec]	2410	2426	4096	2682
Cycle distance [km]	35.9	25.1	102.9	39.0
Avg. vehicle speed [km/h]	53.6	37.3	90.5	52.4
Max. vehicle speed [km/h]	124.7	113.5	128.9	130.1
Avg. RPA [1] [m/s^2]	0.29	0.33	0.22	0.44
Characteristic Power [m^2/s^3]	-	-	-	-
Share [%] (*time based*)				
- idling (≤2 km/h)	16.8	21.5	5.2	12.9
- low speed (>2≤50 km/h)	33.8	43.0	14.2	34.0
- medium speed (>50≤90 km/h)	27.8	28.0	10.0	41.5
- high speed (>90 km/h)	21.7	7.5	70.6	11.6

[1] *RPA - relative positive acceleration*

3.2.2 Vehicle On-Road Test Routes

The vehicles were operated over two pre-defined test routes within the greater Morgantown metropolitan area that were aimed at providing a rich diversity of topological characteristics and driving patterns. In particular, the routes can be split into four categories, including i) *highway operation*, characterized by sustained high-speed driving, ii) *urban driving*, characterized by low vehicle speeds and frequent stop and go, iii) *rural driving*, medium vehicle speed operation with occasional stops in the suburban areas, and finally iv) *uphill/downhill* driving, characterized by steeper than usual road grades and medium to higher speed vehicle operation.

The first test route, herein referred to as '*Morgantown Route*' (or MGW Route), comprises a mix of urban driving in downtown Morgantown, WV, and suburban driving conditions in the outskirts of Morgantown with a short portion of interstate operation. The second test route, herein referred to as '*Bruceton Mills Route*', is characterized by predominant high-speed interstate-type operation, including a steeper hill-climb section with an elevation change of ~400m over a distance of 8km (i.e. consistent road grade of ~5%). A summary of average road characteristics is given in Table 3.6 with detailed information for each of the two routes discussed in the following.

1) Route 1: urban and suburban driving => '*Morgantown Route*'
2) Route 2: highway and uphill/downhill driving => '*Bruceton Mills Route*'

Table 3.6: Comparison of test route and driving characteristics; upper and lower range bounds are represented by 1σ.

Cycle	Morgantown Route	Bruceton Mills Route
Cycle duration [sec]	3021 ± *168*	3269 ± *166*
Cycle distance [km]	40 ± *0.02*	80 ± *0.02*
Avg. vehicle speed [km/h]	48 ± *2.7*	88 ± *4.2*
Max. vehicle speed [km/h]	122 ± *3.8*	127 ± *3.4*
Avg. RPA [1)] [m/s^2]	0.28 ± *0.01*	0.24 ± *0.03*
Characteristic Power [m^2/s^3]	2.31 ± *0.22*	3.26 ± *0.19*
Share [%] (*time based*)		
- idling (≤2 km/h)	18 ± *2.6*	9 ± *2.6*
- low speed (>2≤50 km/h)	41 ± *3.9*	12 ± *1.2*
- medium speed (>50≤90 km/h)	24 ± *2.7*	12 ± *0.6*
- high speed (>90 km/h)	17 ± *1.1*	66 ± *2.7*

[1)] *RPA - relative positive acceleration*

Route and driving characteristics provided in Table 3.6 are representative of typical week-day driving conditions for the urban routes (i.e. MGW route), and non-rush-hour, week-day driving conditions for highway driving (i.e. Bruceton Mills route). Relative positive acceleration (RPA) is a frequently used metric for analysis of route characteristics [7]. '*Characteristic Power*' is a metric derived by Delgado et al. [8, 9] taking kinematic power and grade changes over the driving route into account, and is representative of the positive mechanical energy supplied per unit mass and unit time. Delgado et al. [8, 9] described '*Characteristic Power*' as outlined in Equation 3 having units [m2/s3 or W/kg] with 'T' being the duration of the route, 'g' the gravitational acceleration (i.e. 9.81m/s2), 'v_i' and 'h_i' being the vehicle speed and altitude at each time step, respectively.

$$P_{ch} = \frac{1}{T} \cdot \sum_{i=2}^{N} \left[\frac{1}{2} \cdot (v_i^2 - v_{i-1}^2) + g \cdot (h_i - h_{i-1}) \right]^{+} \qquad \textbf{Eq. 3}$$

For comparison reason with the on-road test routes, Table 3.4 and Table 3.5 provide a summary containing the same metrics as shown in Table 3.6 for a set of chassis dynamometer vehicle certification test cycles that are currently used by the US EPA (FTP-75, US06, SC03) and the European Union (NEDC, WLTP). It can be noticed that the US06 and HWFET cycles shows similar maximum and average speed patterns as the highway (i.e. Bruceton Mills), whereas the FTP-75 closer represents maximum and average speed characteristics of the urban test route (i.e. MGW route).

3.2.2.1 Morgantown Route - urban/suburban driving

The Morgantown route circles around the city of Morgantown, WV and covers several aspects encountered in real-world driving. It consisted of rural driving, urban driving, and highway driving. The route started at WVU's Engineering Campus and continues to southbound I-79. The route continues and merges onto eastbound I-68. From I-68, exit 4 toward Sabraton is taken and continues along WV Route 7. The next exchange is a right-hand turn onto County Road 857 towards US 119, the Mileground Road. Next the route continues southwest on US 119 until it intersects with Route 705. Route 705 is followed back to the WVU Engineering Campus. Figure 3.1 shows the topographic map of the route whereas Figure 3.2 depicts the typical vehicle speed pattern plotted versus the route duration.

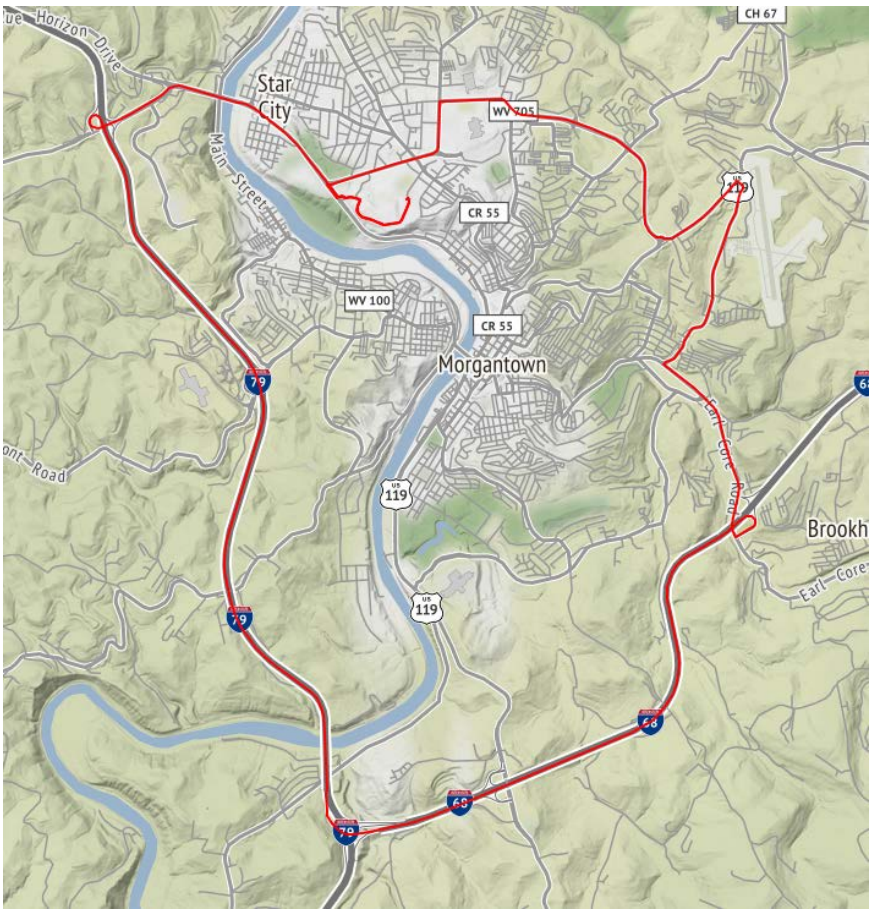

Figure 3.1: Topographic map of Morgantown route, mix of urban, suburban and highway driving around Morgantown, WV.

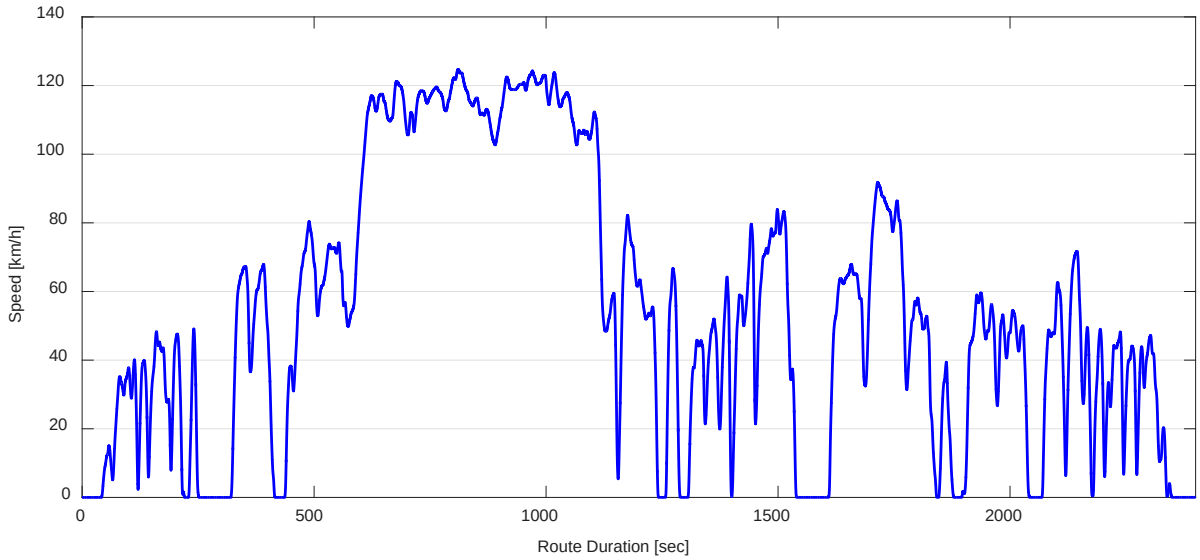

Figure 3.2: Characteristic vehicle speed vs. time for the Morgantown route.

3.2.2.2 Bruceton Mills Route - highway and up/downhill driving

This route represents vehicle operation on a freeway characterized by steep gradients. Interstate I-68 originates/terminates in Morgantown and runs for a total distance of 113 miles through the Appalachian mountain range to/from the intersection of I-70 near Hancock, MD. The proposed test route consists of a 30 mile stretch on interstate 68 between Morgantown, WV (Engineering Campus) and Bruceton Mills, WV. The interstate is characterized by a higher speed limit of 70mph, hence, representing an increased vehicle speed as well as elevated up-/downhill type operation. Figure 3.3 shows the topographic map of the route whereas Figure 3.4 depicts the typical vehicle speed pattern plotted versus the route duration.

Figure 3.3: Topographic map of Bruceton Mills route, highway driving with increased road gradients between Morgantown, WV and Bruceton Mills, WV.

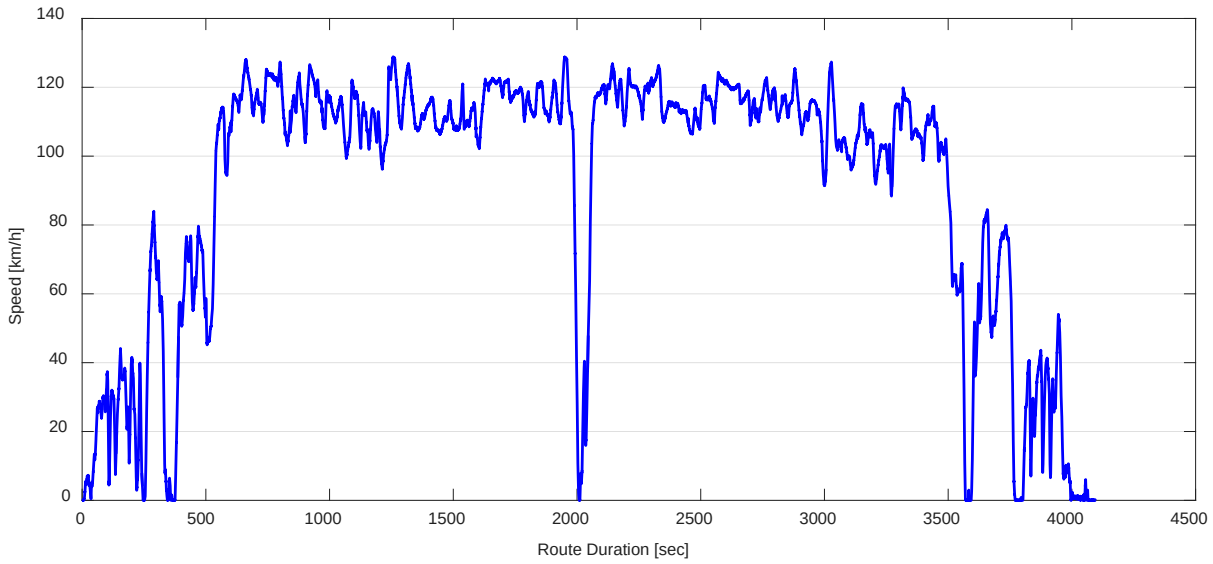

Figure 3.4: Characteristic vehicle speed vs. time for the Bruceton Mills route.

The highway (i.e. Bruceton Mills) driving route experienced an elevation change of approximately 600 meters. The primary measure of altitude during the course of this study was the GPS signal. However, due to sporadically deteriorating GPS reception, caused by a multitude of factors, including but not limited to heavy cloud overcast, road tunnels and underpasses (e.g. bridges), as well as high buildings in downtown areas, an alternative backup method to calculate altitude was employed by means of measuring changes in barometric pressure as a function of altitude using a high resolution pressure transducer. The latter method has proven, during previous studies at WVU [8, 11], to be more accurate for the purpose of calculating road grade changes, however, it is plagued by the requirement to consider local weather conditions as changes in

environmental conditions will lead to changing barometric pressures, hence, offset the altitude calculation.

Equation 4 shows a simplified version of the formula used to calculate altitude '*H*' as a function of reference temperature 'T_0' and pressure 'p_0' at ground level as well as the actually measured barometric pressure 'p_{baro}'. With '*L*' being the temperature lapse rate, 0.0065K/m, and *g*, *M*, *R* being the gravitational acceleration, molar mass of dry air and universal gas constant, respectively [11]. Equation 3 is derived from the International Standard Atmosphere (ISA) model which has been formulated by the International Civil Aviation Organization (ICAO) and is based on assuming ideal gas, gravity independence of altitude, hydrostatic equilibrium, and a constant lapse rate [8].

$$H = f(T_0, p_0, p_{baro}) = \left(\frac{T_0}{L}\right) \cdot \left[1 - \left(\frac{p_{baro}}{p_0}\right)^{\left[\frac{R \cdot L}{g \cdot M_{air}}\right]}\right] \qquad \textbf{Eq. 4}$$

Relative positive acceleration (RPA) is a frequently used metric [7] for the analysis of driving patterns and as input parameter to aid in developing chassis dynamometer test cycles representative of real-world driving. The RPA is calculated as the integral of the product of vehicle speed and positive acceleration for each instance in time, over a given '*micro-trip*' of the test route under investigation as shown by Equation 5. For this study a '*micro-trip*' was defined following the same convention as proposed by Weiss *et al.* [-] as any portion of the test route, where the vehicle speed is equal or larger than 2 km/h for a duration of at least 5 seconds or more. Instantaneous vehicle acceleration was calculated according to Equation 6 by means of differentiating vehicle speed data collected via GPS, and subsequently filtered with negative values being forced to zero.

$$RPA = \frac{\int_0^{t_j} (v_i \cdot a_i) dt}{x_j} \qquad \textbf{Eq. 5}$$

where: t_j duration of micro-trip *j*

x_j distance of micro-trip *j*

v_i speed during each time increment *i*

a_i instantaneous positive acceleration during each time increment *i* contained in the micro-trip *j*

$$a_i = \begin{cases} \dfrac{(v_2 - v_1)}{(t_2 - t_1)} & if\ i = 1 \\ \dfrac{(v_{i+1} - v_{i-1})}{(t_{i+1} - t_{i-1})} & if\ 2 \leq i \leq n-1 \\ \dfrac{(v_n - v_{n-1})}{(t_n - t_{n-1})} & if\ i = n \end{cases} \qquad \textbf{Eq. 6}$$

3.3 Emissions Testing Procedure and PEMS Equipment

The emissions sampling setup employed during the course of this work comprised two measurement sub-systems as shown in the schematic in Figure 3.5. Gaseous exhaust emissions were quantified using the on-board measurement system, OBS-ONE, from Horiba® described in more detail in Section 3.3.1, whereas real-time particle number concentration measurements were performed using the Pegasor particle sensor (PPS), model PPS-M from Pegasor Ltd. discussed in Section 3.3.2. The Horiba OBS-ONE PEMS system is compliant with requirements set forth by CFR, title 40, part 86 and 1065 for the US-EPA heavy-duty in-use emissions compliance program as well as with European EU 582/2011 in-use emissions measurement requirements.

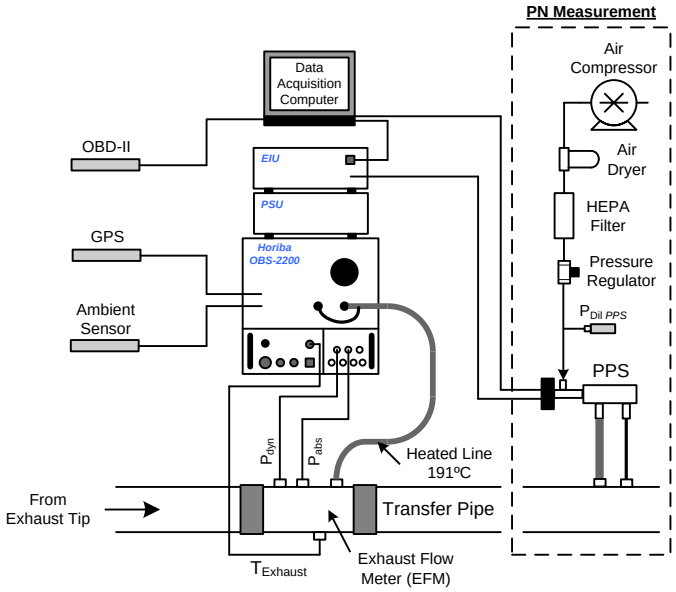

Figure 3.5: Schematic of measurement setup for gaseous and particle phase emissions

Table 3.7 lists all the parameters and emissions constituents collected during this work. Emissions parameters along with GPS and ECU data were sampled and stored continuously at 10Hz frequency by the Horiba® OBS-ONE system. An external sensor, remotely located on the test vehicle's roof, was used to measure ambient conditions, including temperature, barometric pressure and relative humidity, feeding data directly to the OBS-ONE data acquisition software. Vehicle position (i.e. longitude, latitude and altitude) and relative speed were measured by means of a GPS receiver, allowing for subsequent calculation of instantaneous vehicle acceleration and distance traveled (i.e. part of OBS-ONE system).

Engine specific parameters were recorded from publicly broadcasted ECU signals through the vehicles OBD-II port using a CAN adapter, and were feeding directly into the OBS-ONE data acquisition system. Logged parameters included, but were not limited to, engine speed and load, intake air mass flow rate, engine fuel rate, and exhaust temperatures.

Table 3.7: Overview of measured parameters and respective instruments/analyzers

Category	Parameter	Measurement Technique
Exhaust gas pollutants	CO [%]	NDIR (Horiba OBS-ONE)
	CO_2 [%]	NDIR (Horiba OBS- ONE)
	NO_x [ppm]	CLD (Horiba OBS- ONE)
	NO [ppm]	CLD (Horiba OBS- ONE)
	H_2O [%]	NDIR (Horiba OBS-ONE)
Exhaust flow	Exhaust flow rate [m^3/min]	EFM (Horiba OBS-ONE)
	Exhaust temperature [°C]	EFM, K-type thermocouple
	Exhaust absolute pressure [kPa]	EFM (Horiba OBS-ONE)
Exhaust PN/PM emissions	PN concentration [#/cm^3]	Pegasor Particle Sensor
Ambient conditions	Ambient temperature [°C]	Temp. Sensor (OBS-ONE)
	Ambient humidity [%]	Humidity Sensor (OBS-ONE)
	Barometric pressure [kPa]	Pressure Sensor (OBS-ONE)
Vehicle/route characteristics	Vehicle speed [km/h]	GPS (OBS-ONE)
	Vehicle position [°]	GPS (OBS-ONE)
	Vehicle altitude [m a.s.l.]	GPS (OBS-ONE)
	Vehicle acceleration [m/s^2]	Derived from GPS data
	Vehicle distance traveled [km]	Derived from GPS data
Engine characteristics	Engine speed [rpm]	ECU OBD-II (OBS-ONE)
	Engine load [%]	ECU OBD-II (OBS-ONE)
	Engine coolant temperature [°C]	ECU OBD-II (OBS-ONE)
	Engine intake air flow [kg/min]	ECU OBD-II (OBS-ONE)
	Exhaust temperature [°C]	ECU OBD-II (OBS-ONE)

3.3.1 Gaseous Emissions Sampling – Horiba® OBS-ONE

Gaseous raw emissions, including CO, NO, NO_x, THC as well as CO_2 were measured on a continuous basis using the Horiba® OBS-ONE on-board emissions measurement system which has been specifically developed with regard to PEMS requirements for on-road vehicle emissions testing according to recommendations outlined in CFR, Title 40, Part 1065. The emissions of CO and CO_2 were measured using a non-dispersive infrared (NDIR) spectrometer (heated wet sample), THC using a flame ionization detector (FID) (heated wet sample), and NO and total NO_x using a

chemiluminescence detector (CLD) in conjunction with an NO_2-to-NO converter (heated wet sample).

Gaseous emissions were extracted by means of an averaging sample probe through a ½" NPT port installed on the exhaust flow meter adapter that was mounted to the exhaust end pipe. The exhaust sample was directed through a heated line, maintained at a nominal temperature of 191°C using a PID-type controller, to the analyzer inlet port.

The exhaust flow meter (EFM), used in conjunction with the OBS-ONE instrument is a Pitot-tube type flow meter involving the measurement of dynamic and static pressure heads by means of differential and absolute pressure transducers. The fluid temperature (exhaust gas) is measured via a K-type thermocouple allowing to adjust the exhaust gas flow measurement to EPA defined standard conditions (i.e. 293.15K and 101.325 kPa). Additional to pressure and thermocouple ports the EFM adapter features a port for connecting the exhaust gas sampling probe. An averaging type probe with multiple holes spanning the entire EFM adapter's diameter was used to extract continuous exhaust samples.

3.3.2 PEMS Particle Mass/Number Measurements with Pegasor Particle Sensor

Particle number concentration measurements were performed using the Pegasor particle sensor, model PPS-M from Pegasor Ltd. (Finland) [21] which is capable of performing continuous measurements directly in the exhaust stack and providing a real-time signal with a frequency response of up to 100Hz (see Figure 3.6). The sensor operates as diffusion-charging (DC) type device and measures PM based on the current induced by the charged particles leaving the sensor. Figure 3.7 shows the PPS as well as the sample gas flow paths. Dry, HEPA filtered dilution air is supplied at about 22psi and subsequently charged by a unipolar corona discharge charger using a tungsten wire at ~2kV and 5µA. The pressurized dilution air, carrying the unipolar ions, then draws raw exhaust gas through an ejector-type diluter into a mixing chamber, where the ions are turbulently mixed with exhaust aerosol particles for diffusion charging. The sample gas flow is controlled by means of a critical flow orifice and is a function of the supplied dilution air pressure. An electrostatic precipitator (ion trap), installed downstream of the mixing chamber and operating at a moderate voltage of approximately 100V, traps excess ions that escaped the charging zone. Finally, the charge of the out-flowing particles is measured using a built-in electrometer. The measured current signal is amplified and filtered by the internal electronic control unit of the sensor

and outputted either as a voltage or current value. The sensors output can be subsequently correlated to other aerosol instruments by means of linear regression in order to measure the concentration of the mass, surface or number of the exhaust particles, depending on the chosen reference instrument.

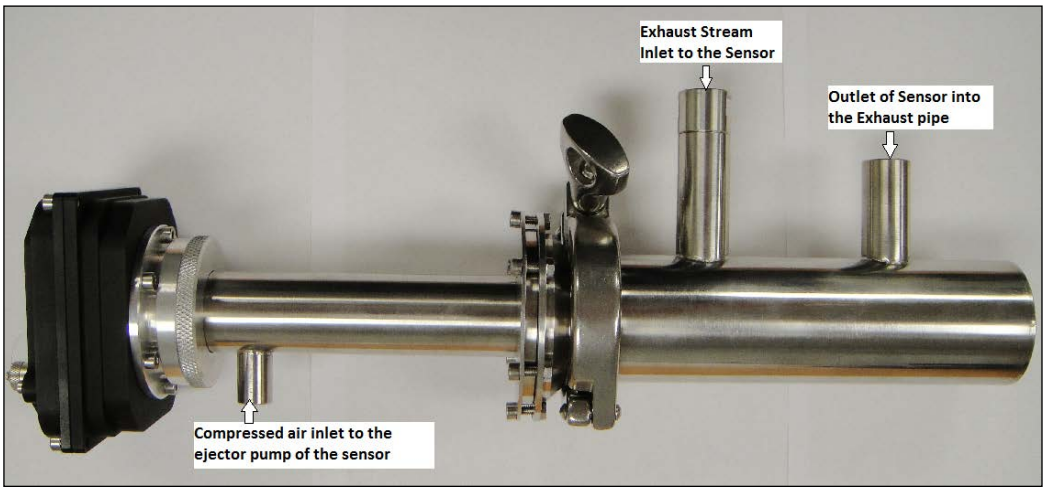

Figure 3.6: Pegasor particle sensor, model PPS-M from Pegasor Ltd. (Finland)

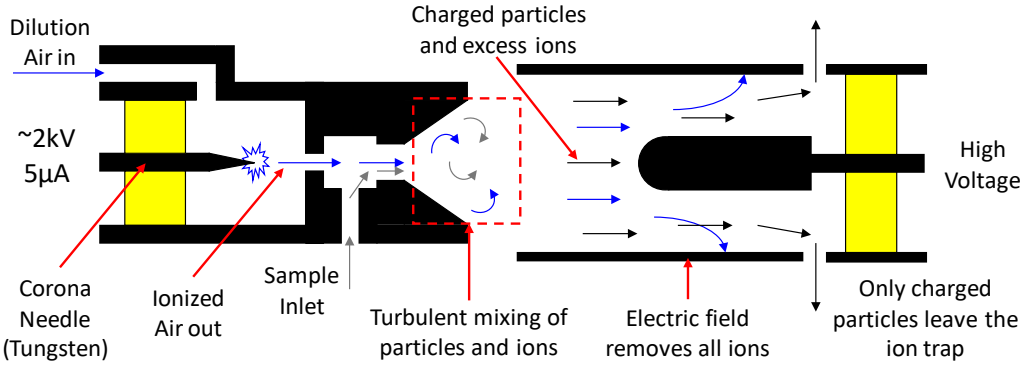

Figure 3.7: PPS measurement principle with sample gas and dilution air flow paths [22, 23]

Extensive testing of this sensor at the engine testing facility at WVU, has shown the capability of this sensor to accurately measure the total PM concentration in comparison to other standard aerosol instruments such as the Ultrafine Condensation Particle Counter (TSI UCPC, Model 3025), the Engine Exhaust Particle Sizer spectrometer (TSI EEPS™, Model 3090) as well as the Micro-Soot Sensor (MSS) from AVL (Model 483) [23]. The sensor was designed as a flow through device and therefore does not involve collection or contact with particles in the exhaust stream, which is especially advantageous for long-term stability and operation without frequent maintenance; hence, best suited for in-use application.

3.3.3 PEMS Verification and Pre-test Checks

3.3.3.1 PEMS Verification and Analyzer Checks

In-Use testing begins by verifying the correct operation of testing equipment, according to CFR, Title 40, Part 1065, Subparts D and J. This involves preparation and installation the portable emissions measurement equipment, with requisite gases and all ancillary hardware pertaining to the system, and allowing the equipment to reach operating temperature, generally after 1-2 hours.

After warm-up, the inspection begins with setting span concentrations to the correct levels based on the calibration cylinder used, ensuring concentrations are entered on the ranges to be used during the actual testing. Before generating any linearization curves, a simple zero and span (calibration) of the analyzers is performed.

Along with monthly and yearly checks to be described later, many PEMS manufacturers, such as Horiba® Instruments, also recommend monthly adjustments to be performed on analyzers, namely the "amplifier zero" and "detector gain" adjustments for Flame Ionization Detectors (FID) and Chemiluminescence Detector (CLD) analyzers, and the "amplifier gain" for the FID analyzer. These adjustments affect the sensitivity of the FID and CLD analyzers, and should be performed prior to any other system checks.

After performing analyzer detector adjustments, calibration curves must be generated for each analyzer by measuring the analyzer raw response to calibration gas blended over at least 10 points and performing a least squares fit through the data (40 CFR 1065.307). At the end of the "linearization" verification procedure, determine whether curves meet applicable specifications.

Once satisfactory performance of the gas analyzers has been obtained at the calibration and linearization levels, the next step is to perform interference checks. These checks quantify the amount of interference between the component being measured and any other components that are known to interfere with its measurement and that are ordinarily present in the sample. Ultimately, it is up to the operator to decide whether the amount of interference is within acceptable limits, although Horiba OBS automated procedures help guide the operator through this process with a routine that compares interference results against pre-determined limits based on 40 CFR 1065 Subpart D.

NOx converter efficiency and Oxygen interference on the FID must also be checked according to 40 CFR 1065.362 and 1065.378 to ensure valid test results.

The heated sample line must also be checked for proper operation, specifically for any leaks in the system, and for proper control of the heated surfaces. Leak checks are easily performed via a vacuum-side leak verification (40 CFR 1065.345), using a pressure calibration device, and temperature traces can be established with a thermocouple and thermocouple calibrator.

The exhaust flow measurement (EFM) unit will be verified against in a flow bench with a laminar flow element that is calibrated against NIST traceable standards in order to verify the flow as measured by the PEMS unit.

PM measurement equipment must also be verified according to manufacturer recommendations and good engineering judgment. Ordinarily, this involves various leak checks and sample flow checks using calibrated flow meters.

Upon completion of PEMS system checks and linearization, a WVU QA officer will review the results of these checks and decide whether testing is to proceed.

3.3.3.2 1.4.2 PEMS Installation and Testing

Once all equipment has been verified for field testing, the PEMS equipment will be installed onboard the test vehicle along with the power unit also making sure that the total test vehicle weight does not exceed the GVWR of the vehicle. During the installation, a competent technician will check the condition of the test vehicle for an initial assessment of its test-worthiness. The engine's warranty download and fault codes will be reviewed at this time. Engine oil samples and fuel samples would also be procured at this time. After the installation, but prior to testing, the PEMS equipment is validated by placing all systems in sample with the test vehicle in idle operation. During this time, each measurement will be checked for reasonableness, using good engineering judgment.

Pictures of the test apparatus as it is installed on the vehicle will be taken at this time, along with pictures of identifying badges on the vehicle's engine and VIN plate. A picture of the odometer reading is required both prior to and following the test to document actual vehicle mileage accrued during the test. This mileage should later be compared to the total mileage as measured by the PEMS equipment.

Prior to the beginning of the test, the PEMS equipment will be allowed to run for at least half an hour followed by any final system checks and calibrations. Weather and other environmental conditions should be noted at the beginning and end of the test.

Data will be monitored periodically during the test either through a wireless connection or data can be transferred from the test vehicle during a scheduled stop. It is imperative to the timeliness of the completion of the testing that data be reviewed as quickly as is practical, due to the occasional failure or malfunction of components. The earlier these malfunctions are detected, the sooner they can be rectified and testing resumed.

Review of the data involves a combination of approaches with the first being the use the post processing software supplied by the PEMS manufacturer. In addition, WVU uses in-house software to view graphically continuous (10 Hz) data collected during in-use testing. Every parameter logged will be considered in this review for reasonableness using good engineering judgment. The maximum, minimum and average values of these parameters will all be considered, paying particular attention to discontinuities or lapses in the data. Non-idle operation requirements must be considered alongside in-depth data analysis. Once the data has been thoroughly reviewed and is considered valid, the PEMS can be removed from the test vehicle.

4 RESULTS AND DISCUSSION

The results chapter will discuss the averaged emissions for the criteria pollutants and CO_2 from all Fiat Chrysler Automobiles test vehicles in Section 4.1 for standard chassis dynamometer test cycles (see Section 4.1.1) as well as for on-road operation over the urban/suburban route (i.e. Route 1) and highway route (i.e. Route 2) (see Section 4.1.2), followed by an in-depth comparison of continuous emissions between the on-road routes and the representative chassis dynamometer cycles in Section 4.2. Section 4.3 will discuss the impact of emissions hardware (i.e. catalyst) and ECU software on emissions rates for a MY 2014 Jeep Grand Cherokee.

This report presents gaseous emissions mass rates in [g/s] and emissions factors in [g/km], along with dimensionless deviation ratios (DR) for each emissions constituent as a measure of how much the actual on-road emissions are deviating from the regulatory limit. The calculation of deviation ratios is given by Equation 11 and follows the upcoming European regulation for '*real driving emissions*' (RDE), where m_{x_i} and $[s(t_{end}) - s(t_{start})]_i$ are the emissions mass and distance traveled for a given averaging window or test route, respectively. $EF_{x\,stand}$ was selected to be the regulatory limit for the respective pollutant as given by Table 4.1.

$$DR_i = \frac{\frac{m_{x_i}}{[s(t_{end}) - s(t_{start})]_i}}{EF_{x_{standard}}} \qquad \textbf{Eq. 11}$$

Table 4.1: Applicable regulatory emissions limits and other relevant vehicle emission reference values; US-EPA Tier2-Bin5 at full useful life (10years/ 120,000 mi) for NO_x, CO, THC (eq. to NMOG), and PM [5]; EPA advertised CO_2 values for each vehicle [1]; Euro 5b/b+ for PN [3]

NO_x [g/km]	CO [g/km]	THC [g/km]	CO_2 [g/km]	PM [g/km]	PN [#/km]
0.043	2.610	0.056	432 (*Jeep*) 461/440 (*Ram, 4WD/2WD*)	0.006	$6.0x10^{11}$

DPF regeneration events occurring during chassis dynamometer or on-road operation of the test vehicles were identified by a simultaneous increase in particle number concentrations as measured with the Pegasor particle sensor and exhaust gas temperatures measured at the exhaust flow meter location. Additionally, during DPF regeneration events, NO_x emissions would significantly increase over normal engine/after-treatment operating conditions. For test runs with

DPF regeneration events exhaust gas temperatures increase to approximately 600°C which is required to initiate the periodic soot oxidation from the surface of the filter substrate. Test containing DPF regeneration events were excluded from the results and analysis discussed hereinafter.

4.1 Cycle and Route Averaged Emissions Results

This chapter will present averaged emissions of NO_x and other criteria pollutants for the test vehicles, calculated over the chassis dynamometer test cycles (see Section 4.1.1) and over the two on-road test routes (see Section 4.1.2).

4.1.1 Emissions over Chassis Dynamometer Test Cycles

Figure 4.1 to Figure 4.6 show distance-specific NO_x emissions factors of the test vehicles over various chassis dynamometer test cycles used for vehicle certification in the US (i.e. FTP-75, US06, SC03, and HWFET), and Europe (i.e. NEDC and WLTP), including two real-word cycles developed by CAFEE (i.e. MGW and LA-4 Cycle). In all figures, variation bars represent ±1σ of repeated tests. For FTP -75 cycles, subscript (*C*) represents a *cold-start* test, whereas subscript (*W*) represents a *warm-start* test that was run subsequent to a regular *cold-start* test.

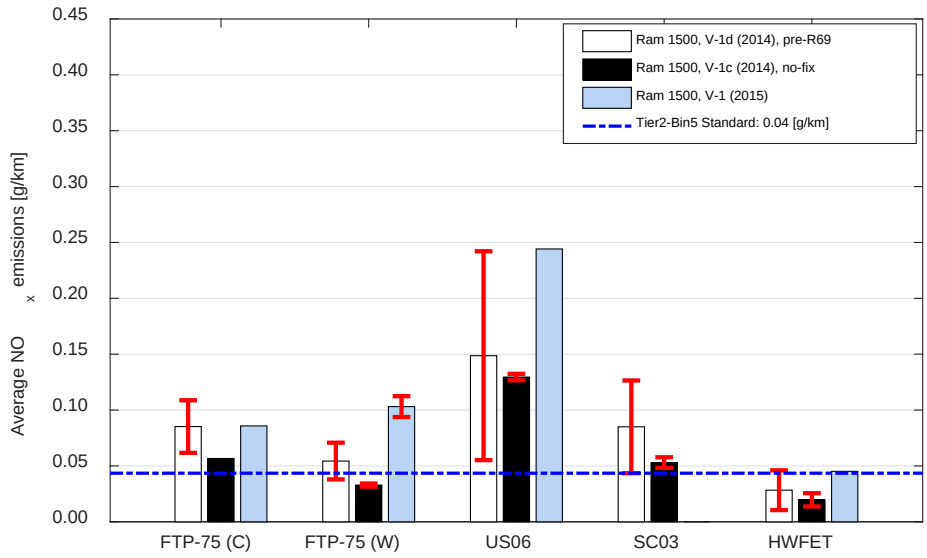

Figure 4.1: Average NO_x emissions of Ram 1500 test vehicles over five standard US-EPA chassis dynamometer test cycles; repeat test variation intervals are presented as ±1σ.

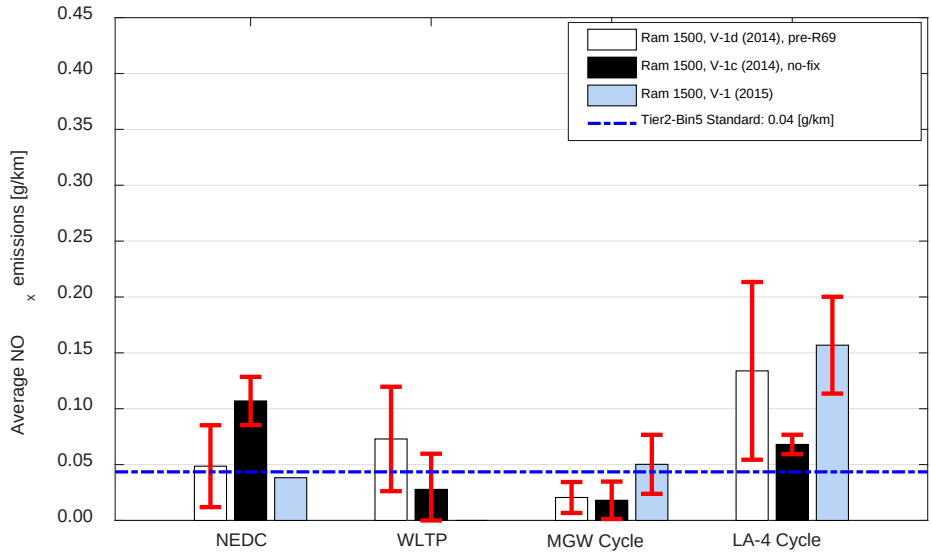

Figure 4.2: Average NO_x emissions of Ram 1500 test vehicles over two standard EU chassis dynamometer test cycles and two real-world cycles (i.e. MGW, LA-4); repeat test variation intervals are presented as ±1σ.

Table 4.2: Average NO_x emissions in [g/km] for all Ram 1500 test vehicles over six standard chassis dynamometer test cycles and two real-world cycles.

Cycle		V-1d (2014)	V-1c (2014)	V-1 (2015)
FTP-75 (Cold)	**μ**	**0.0852**	**0.0567**	**0.0858**
	σ	*0.0235*	-	-
FTP-75 (Warm)	**μ**	**0.0544**	**0.0328**	**0.1031**
	σ	*0.0164*	*0.0014*	*0.0093*
US06 (*highway cycle*)	**μ**	**0.1486**	**0.1295**	**0.2442**
	σ	*0.0935*	*0.0029*	-
SC03	**μ**	**0.0850**	**0.0530**	-
	σ	*0.0415*	*0.0047*	-
HWFET (*highway cycle*)	**μ**	**0.0283**	**0.0197**	**0.0451**
	σ	*0.0178*	*0.0059*	-
NEDC (*Europe*)	**μ**	**0.0486**	**0.1070**	**0.0383**
	σ	*0.0367*	*0.0216*	-
WLTP (*Europe*)	**μ**	**0.0729**	**0.0278**	-
	σ	*0.0467*	*0.0319*	-
MGW Cycle (*real-world cycle*)	**μ**	**0.0206**	**0.0181**	**0.0502**
	σ	*0.0138*	*0.0167*	*0.0264*
LA-4 Cycle (*real-world cycle*)	**μ**	**0.1339**	**0.0680**	**0.1569**
	σ	*0.0795*	*0.0087*	*0.0433*

Note: σ is standard deviation over two consecutive test runs; empty cells indicate no data collected for the given cycle.

Figure 4.1 shows average NO_x emissions factors for all Ram 1500 vehicles tested (incl. MY 2014 and 2015), over five standard chassis dynamometer test cycles that are used in the United States for light-duty vehicle certification. Similarly, Figure 4.2 depicts average NO_x emissions factors for the same test vehicles (i.e. Ram 1500) over the two standard EU chassis dynamometer test cycles and two real-world cycles selected for this study. Additionally, Table 4.2 summarizes the NO_x emissions factors measured over all chassis dynamometer cycles for the Ram 1500 test vehicles.

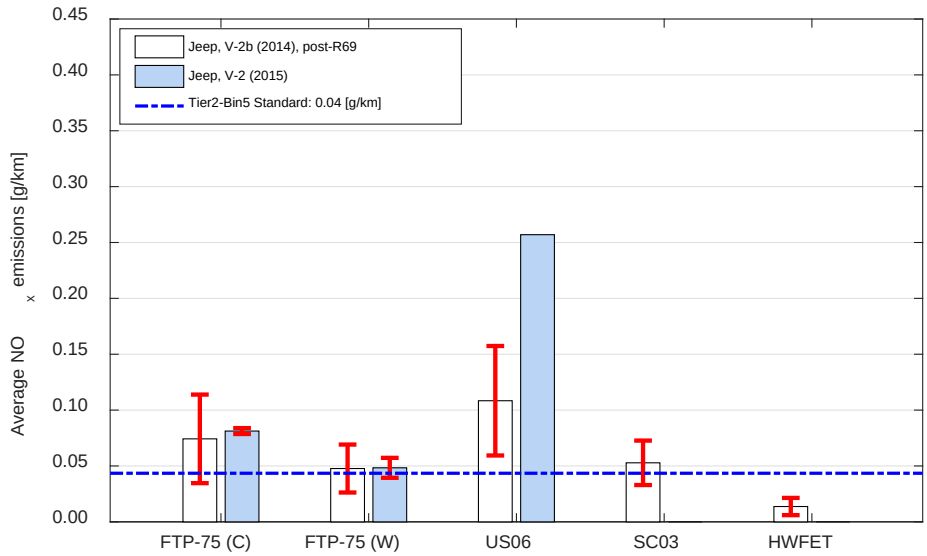

Figure 4.3: Average NO_x emissions of Jeep Grand Cherokee test vehicles over five standard US-EPA chassis dynamometer test cycles; repeat test variation intervals are presented as ±1σ.

Figure 4.3 shows average NO_x emissions factors for Jeep Grand Cherokee vehicles tested (incl. MY 2014 and 2015) over five standard chassis dynamometer test cycles that are used in the United States for light-duty vehicle certification. Analogously, Figure 4.4 depicts average NO_x emissions factors for the same test vehicles (i.e. Jeep Grand Cherokee) over the two standard EU chassis dynamometer test cycles and two real-world cycles selected for this study. It has to be noted, that missing data indicate that a specific test vehicle was not operated over a given test cycle. Additionally, Table 4.3 summarizes the NO_x emissions factors measured over all chassis dynamometer cycles for the Jeep Grand Cherokee test vehicles.

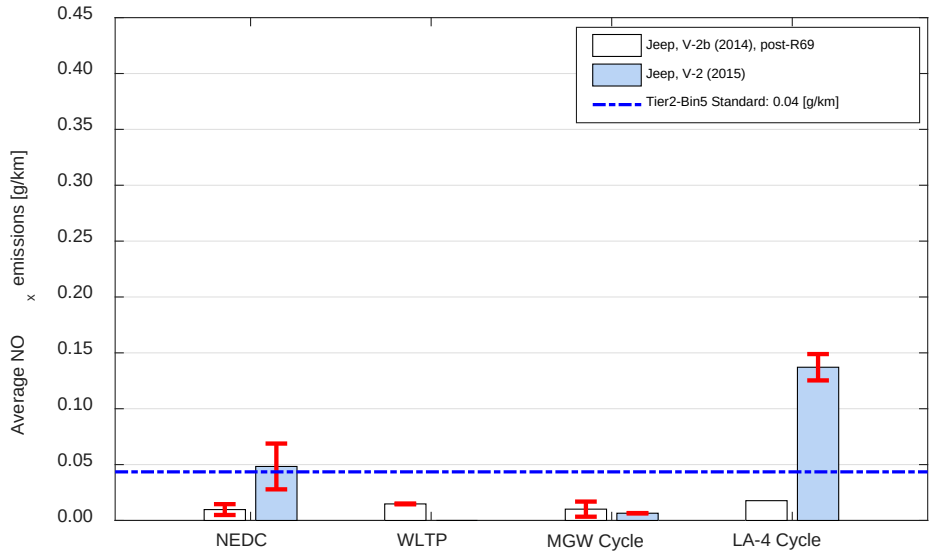

Figure 4.4: Average NO_x emissions of Jeep Grand Cherokee test vehicles over two standard EU chassis dynamometer test cycles and two real-world cycles;

Table 4.3: Average NO_x emissions in [g/km] for all Jeep Grand Cherokee test vehicles over six standard chassis dynamometer test cycles and two real-world cycles.

Cycle		V-2b [1] (2014)	V-2 (2015)
FTP-75 (Cold)	**μ**	**0.0743**	**0.0760**
	σ	*0.0396*	*0.0013*
FTP-75 (Warm)	**μ**	**0.0477**	**0.0452**
	σ	*0.0215*	*0.0078*
US06 (*highway cycle*)	**μ**	**0.1084**	**0.2537**
	σ	*0.0490*	
SC03	**μ**	**0.0528**	
	σ	*0.0199*	
HWFET (*highway cycle*)	**μ**	**0.0137**	
	σ	*0.0077*	
NEDC (*Europe*)	**μ**	**0.0097**	**0.0436**
	σ	*0.0049*	*0.0185*
WLTP (*Europe*)	**μ**	**0.0148**	
	σ	*0.0004*	
MGW Cycle (*real-world cycle*)	**μ**	**0.0101**	**0.0063**
	σ	*0.0068*	*0.0001*
LA-4 Cycle (*real-world cycle*)	**μ**	**0.0177**	**0.1346**
	σ	-	*0.0110*

[1] *Data after recall R69 had been conducted by the FCA dealership*

σ is standard deviation over two consecutive test runs; empty cells indicate no data.

Figure 4.5 along with Figure 4.6 present a comparison of average NO_x emissions factors, over standard chassis dynamometer test cycles and two real-world cycles, for the Ram 1500 (MY 2014, Vehicle 1d) before and after the test vehicle had been recalled by the OEM in order to conduct the *R69 service bulletin*. Procedures outline in R69 included the physical change of the SCR catalyst on the affected vehicles.

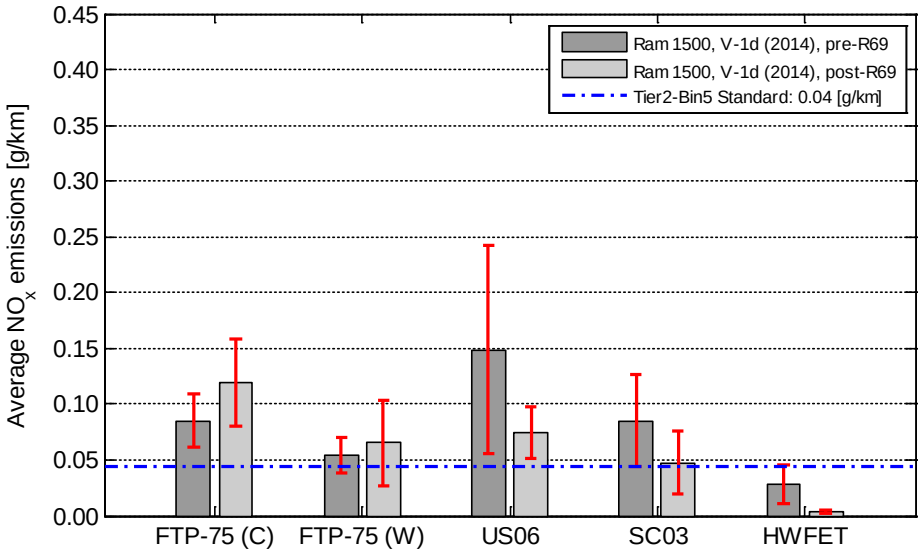

Figure 4.5: Comparison of average NO_x emissions of Ram 1500 (Vehicle 1d), tested before and after recall R69 over five standard US-EPA chassis dynamometer test cycles; repeat test variation intervals are presented as ±1σ.

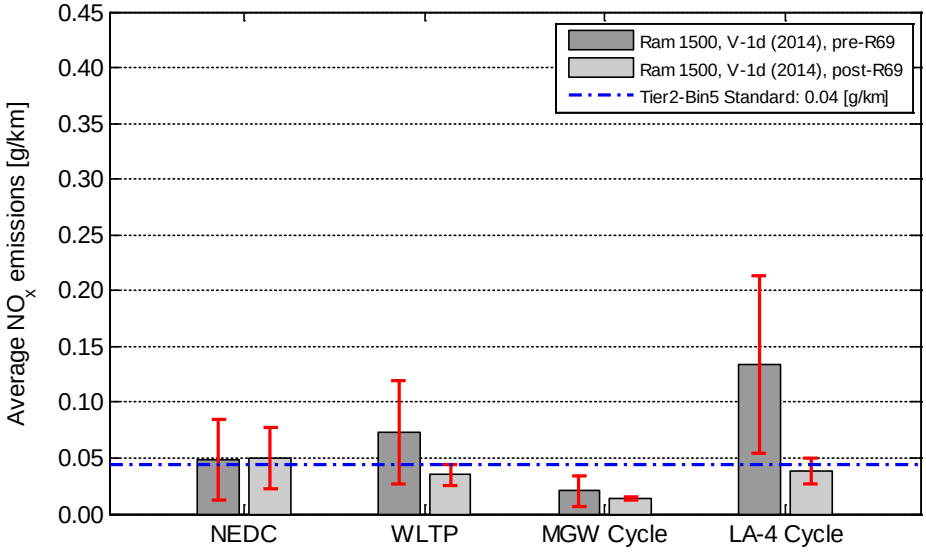

Figure 4.6: Comparison of average NO_x emissions of Ram 1500 (Vehicle 1d), tested before and after recall R69 over two standard EU chassis dynamometer test cycles and two real-world cycles (i.e. MGW, LA-4); repeat test variation intervals are presented as ±1σ.

In general, as can be observed from Figure 4.5 and Figure 4.6, NO_x emissions from chassis dynamometer testing post recall were observed at similar or slightly lower (i.e. with the exception of the FTP-75 cycle) levels than before conducting the recall. Test-to-test variability (i.e. presented by test variation intervals) was seen to reduce after the recall. Table 4.4 summarized chassis dynamometer test results between pre-/post-recall testing conditions.

Table 4.4: Comparison of average NO_x emissions in [g/km] Ram 1500 (Vehicle 1d), tested before and after recall R69, over six standard chassis dynamometer test cycles and two real-world cycles.

Cycle		Pre-Recall	Post-Recall	Δ [%]
FTP-75 (Cold)	**μ**	**0.0852**	**0.1191**	**-39.8**
	σ	*0.0235*	*0.0389*	
FTP-75 (Warm)	**μ**	**0.0544**	**0.0655**	**-20.4**
	σ	*0.0164*	*0.0384*	
US06 (*highway cycle*)	**μ**	**0.1486**	**0.0745**	**32.9**
	σ	*0.0935*	*0.0231*	
SC03	**μ**	**0.0850**	**0.0475**	**70.9**
	σ	*0.0415*	*0.0282*	
HWFET (*highway cycle*)	**μ**	**0.0283**	**0.0036**	**49.9**
	σ	*0.0178*	*0.0012*	
NEDC (*Europe*)	**μ**	**0.0486**	**0.0504**	**-3.7**
	σ	*0.0367*	*0.0273*	
WLTP (*Europe*)	**μ**	**0.0729**	**0.0348**	**44.1**
	σ	*0.0467*	*0.0091*	
MGW Cycle (*real-world cycle*)	**μ**	**0.0206**	**0.0138**	**52.3**
	σ	*0.0138*	*0.0008*	
LA-4 Cycle (*real-world cycle*)	**μ**	**0.1339**	**0.0390**	**87.4**
	σ	*0.0795*	*0.0116*	

Note: σ is standard deviation over two consecutive test runs; empty cells indicate no data collected for the given cycle.

4.1.2 Emissions over On-Road Driving Routes

This chapter will present average on-road emissions factors for NO_x as measured over two pre-defined test routes for all five test vehicles. Results presented in this chapter are reported as total distance-specific emissions over the respective route. The Morgantown Route (i.e. MGW Rt.) was operated with three different initial vehicle conditioning methods, namely; i) as *cold-start*, after the vehicle had been soaking overnight at ambient room temperature (i.e. indicated by

subscript *C*); ii) as *hot-start*, with the engine remain idling for about 10min after finishing the *cold-start* test and before starting the second test run (i.e. indicated by subscript *H*); and ii) as *warm-start*, with the vehicle soaking for about 10min in '*key-off*' position (i.e. engine off) in between two consecutive test runs (i.e. indicated by subscript *W*).

Figure 4.7 along with Figure 4.8 show average NO_x emissions factors and their respective deviation ratio from the US-EPA Tier2-Bin5 standard, respectively, over the two pre-defined test routes for all Ram 1500 test vehicles (i.e. vehicles 1, 1c, and 1d). Additionally, Table 4.5 and Table 4.6 summarize the average emissions factors, respective standard deviation (1σ) and average deviation ratios from the US-EPA standard computed over repetitions of a given test route.

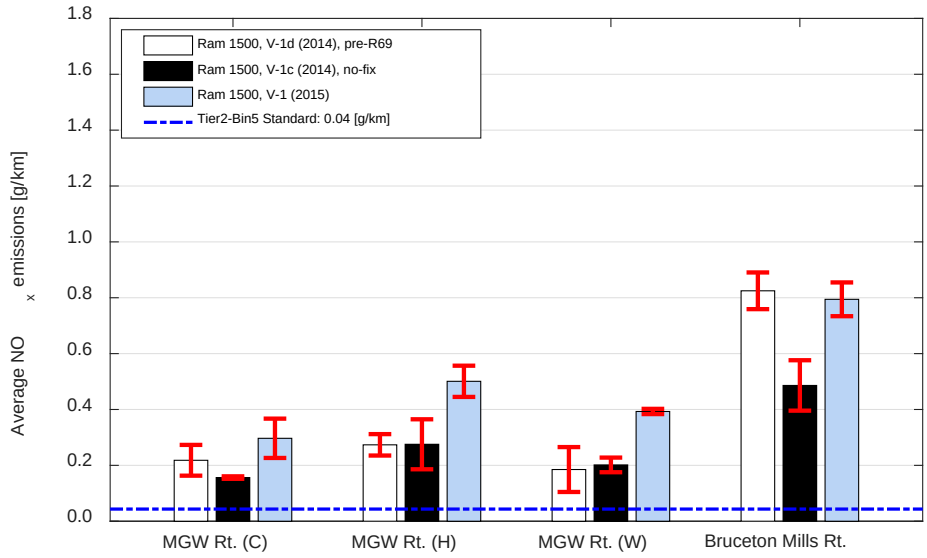

Figure 4.7: Average NO_x emissions of Ram 1500 test vehicles over two on-road driving routes compared to US-EPA Tier2-Bin5 (at full useful life) emissions standard; repeat test variation intervals are presented as ±1σ; MGW Rt. (C) - cold start; MGW Rt. (H) - run as hot start; MGW Rt. (W) - run as warm start after '*key-off*' and ~10min soak time.

In general, NO_x emissions factors were found to be highest for highway driving conditions, which included an up/downhill section, and lowest for rural and urban driving conditions. All three Ram 1500 test vehicles show distinct NO_x emissions patterns, with the pre-recall vehicle 1d exhibiting NO_x emissions 5 to 19, vehicle 1c NO_x emissions 4 to 11, and finally, with vehicle 1 exhibiting NO_x emissions 7 to 18 times the US-EPA Tier2-Bin5 standard depending on the test route.

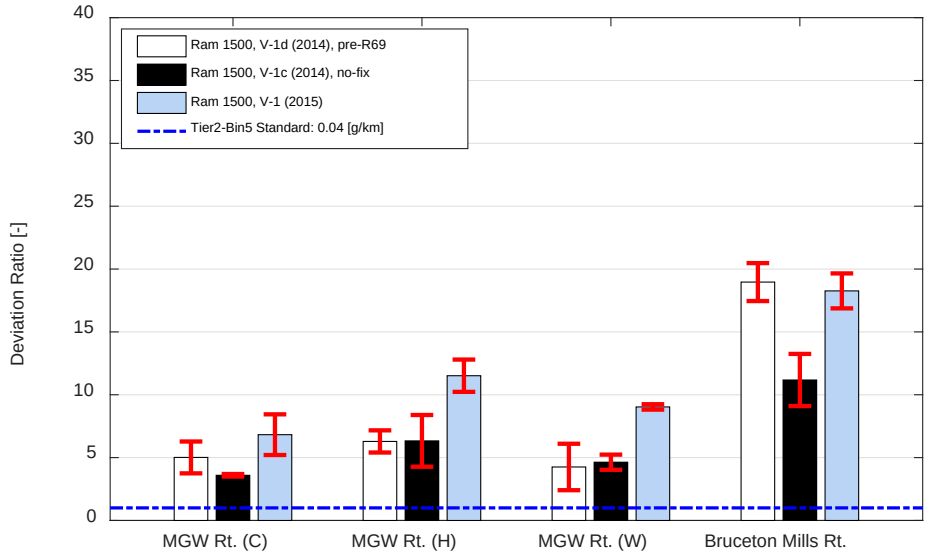

Figure 4.8: Average NO_x emissions of Ram 1500 test vehicles over two on-road driving routes expressed as deviation ratio; repeat test variation intervals are presented as ±1σ.

Table 4.5: Average NO_x emissions in [g/km] for all Ram 1500 test vehicles over two on-road driving routes; σ is standard deviation over consecutive test runs.

Cycle		V-1d (2014)	V-1c (2014)	V-1 (2015)
MGW Rt. (Cold)	**μ**	**0.2181**	**0.1563**	**0.2968**
	σ	*0.0551*	*0.0045*	*0.0704*
MGW Rt. (Hot)	**μ**	**0.2735**	**0.2754**	**0.05009**
	σ	*0.0383*	*0.0895*	*0.0559*
MGW Rt. (Warm)	**μ**	**0.1851**	**0.2016**	**0.3929**
	σ	*0.0804*	*0.0262*	*0.0094*
Bruceton Mills Rt.	**μ**	**0.8249**	**0.4860**	**0.7944**
	σ	*0.0657*	*0.0902*	*0.0605*

Table 4.6: Average NO_x emissions for all Ram 1500 test vehicles over two on-road driving routes expressed as deviation ratio; σ is standard deviation over consecutive test runs.

Cycle		V-1d (2014)	V-1c (2014)	V-1 (2015)
MGW Rt. (Cold)	**μ**	**5.01**	**3.59**	**6.82**
	σ	*1.27*	*0.10*	*1.62*
MGW Rt. (Hot)	**μ**	**6.29**	**6.33**	**11.52**
	σ	*0.88*	*2.06*	*1.28*
MGW Rt. (Warm)	**μ**	**4.25**	**4.63**	**9.03**
	σ	*1.85*	*0.60*	*0.22*
Bruceton Mills Rt.	**μ**	**18.96**	**11.17**	**18.26**

	σ	*1.51*	*2.07*	*1.39*

Figure 4.9 and Figure 4.10 show average NO_x emissions factors and their respective deviation ratio from the US-EPA Tier2-Bin5 standard, respectively, over the two pre-defined test routes for the two Jeep Grand Cherokee test vehicles (i.e. vehicles 2 and 2b). Additionally, Table 4.7 and Table 4.8 summarize the average emissions factors, respective standard deviation (1σ) and average deviation ratios from the US-EPA standard computed over repetitions of a given test route.

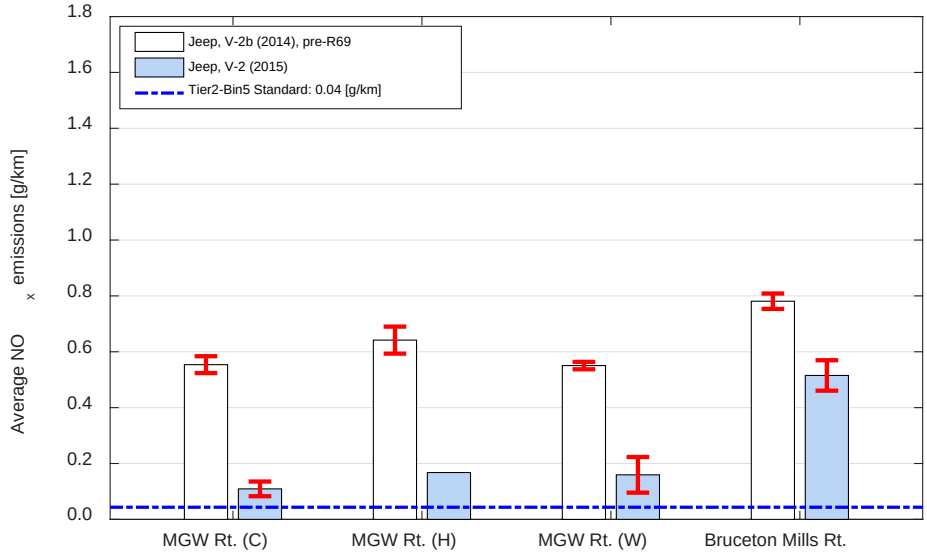

Figure 4.9: Average NO_x emissions of Jeep Grand Cherokee test vehicles over two on-road driving routes compared to US-EPA Tier2-Bin5 (at full useful life) emissions standard; repeat test variation intervals are presented as ±1σ.

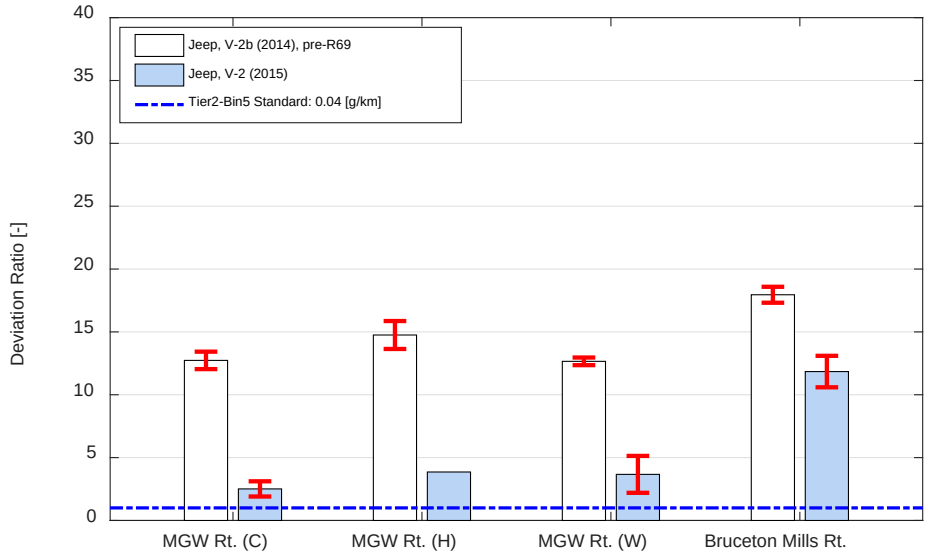

Figure 4.10: Average NO_x emissions of Jeep Grand Cherokee test vehicles over two on-road driving routes expressed as deviation ratio; repeat test variation intervals are presented as ±1σ.

In general, and similarly to results found for Ram 1500 vehicles, NO_x emissions factors from Jeep Grand Cherokee test vehicles were observed to be highest for highway driving conditions, which included an up/downhill section, and lowest for rural and urban driving conditions. All two Jeep Grand Cherokee test vehicles show distinct NO_x emissions patterns, with vehicle 2 exhibiting NO_x emissions 2 to 12 times the US-EPA Tier2-Bin5 standard depending on test route.

Vehicle 2b showed significantly higher NO_x emissions factors with deviation ratios ranging from 12 to 29 during pre-recall conditions. After the vehicle had been subjected to the recall (i.e. R69 service bulletin) NO_x deviation ratios dropped to levels similar to what was observed from the other Jeep in the range of 2 to 12.

Table 4.7: Average NO_x emissions in [g/km] for all Jeep Grand Cherokee test vehicles over two on-road driving routes; σ is standard deviation over consecutive test runs.

Cycle		V-2 (2015)	V-2b (2014)	V-2b (pre-recall) (2014)
MGW Rt. (Cold)	**μ**	**0.1092**	**0.1244**	**0.5739**
	σ	*0.0263*	*0.0294*	-
MGW Rt. (Hot)	**μ**	**0.1677**	**0.0894**	**0.5005**
	σ	-	*0.0348*	-
MGW Rt. (Warm)	**μ**	**0.1595**	**0.1094**	**1.2406**
	σ	*0.0639*	*0.0238*	-
	μ	**0.5152**	**0.5063**	**0.7712**

Bruceton Mills Rt.	*σ*	*0.0545*	*0.0970*	*0.0283*

Table 4.8: Average NO_x emissions for all Jeep Grand Cherokee test vehicles over two on-road driving routes expressed as deviation ratio; σ is standard deviation over consecutive test runs.

Cycle		V-2 (2015)	V-2b (2014)	V-2b (pre-recall) (2014)
MGW Rt. (Cold)	**μ**	**2.51**	**2.86**	**13.19**
	σ	*0.61*	*0.68*	-
MGW Rt. (Hot)	**μ**	**3.86**	**2.06**	**11.51**
	σ	-	*0.80*	-
MGW Rt. (Warm)	**μ**	**3.67**	**2.51**	**28.52**
	σ	*1.47*	*0.55*	-
Bruceton Mills Rt.	**μ**	**11.85**	**11.64**	**17.73**
	σ	*1.25*	*2.23*	*0.65*

Figure 4.11 along with Figure 4.12 show a comparison of average NO_x emissions factors and their respective deviation ratio from the US-EPA Tier2-Bin5 standard, respectively, over the two pre-defined test routes for the Ram 1500 (i.e. vehicle 1d) before and after the vehicle was subjected to the R69 emissions recall. The measured data indicated no statistically significant difference in NO_x emissions over any of the driving conditions investigated in this study, after the recall had been conducted.

In a similar fashion, Figure 4.13 and Figure 4.14 show a comparison of average NO_x emissions factors and their respective deviation ratio from the US-EPA Tier2-Bin5 standard, respectively, over the two pre-defined test routes for the Jeep Grand Cherokee (i.e. vehicle 2b) before and after the vehicle was subjected to the R69 recall. In stark contrast to the Ram 1500 (i.e. vehicle 1d), the Jeep Grand Cherokee showed significantly reduced NO_x emissions after the emissions recall R69 had been conducted by the OEM. Average NO_x emissions reduced by about 80-90% over the urban/suburban driving route (i.e. MGW Rt.) and ~35% during highway driving conditions (i.e. Bruceton Mills Rt.) as compared to pre-recall NO_x emissions factors.

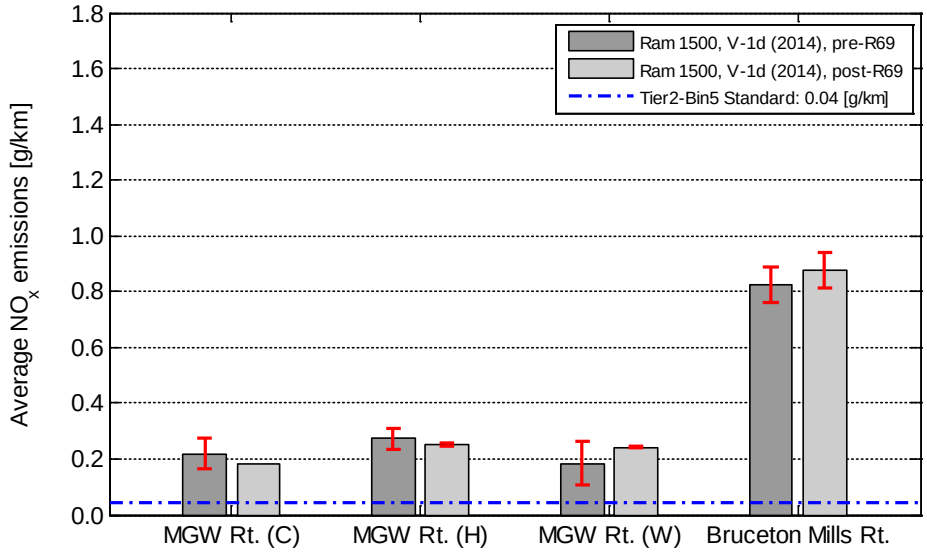

Figure 4.11: Comparison of average NO_x emissions of Ram 1500 (Vehicle 1d), tested before and after recall R69 over two on-road driving routes compared to US-EPA Tier2-Bin5 (at full useful life) emissions standard; repeat test variation intervals are presented as ±1σ; MGW Rt. (C) - cold start; MGW Rt. (H) - run as hot start; MGW Rt. (W) - run as warm start after '*key-off*' and ~10min soak time.

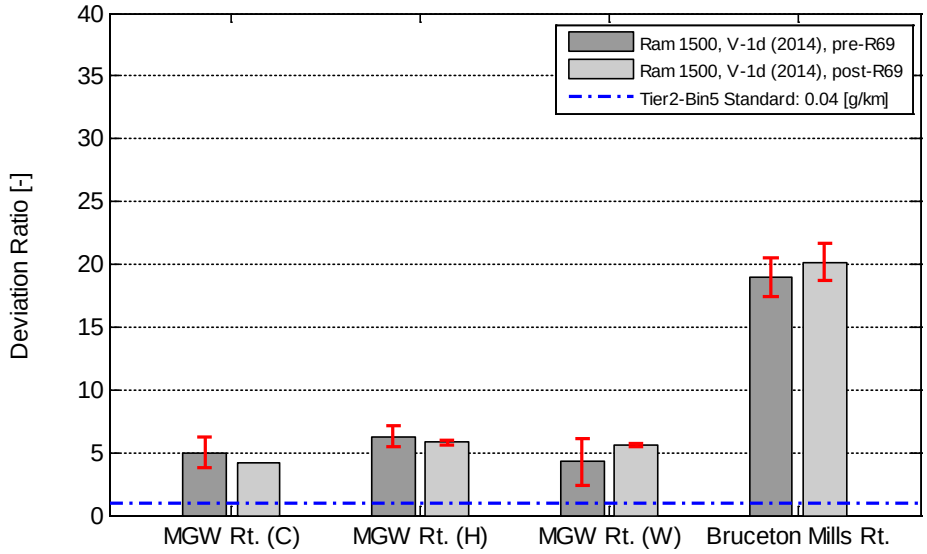

Figure 4.12: Comparison of average NO_x emissions of Ram 1500 (Vehicle 1d), tested before and after recall R69 over two on-road driving routes expressed as deviation ratio; repeat test variation intervals are presented as ±1σ.

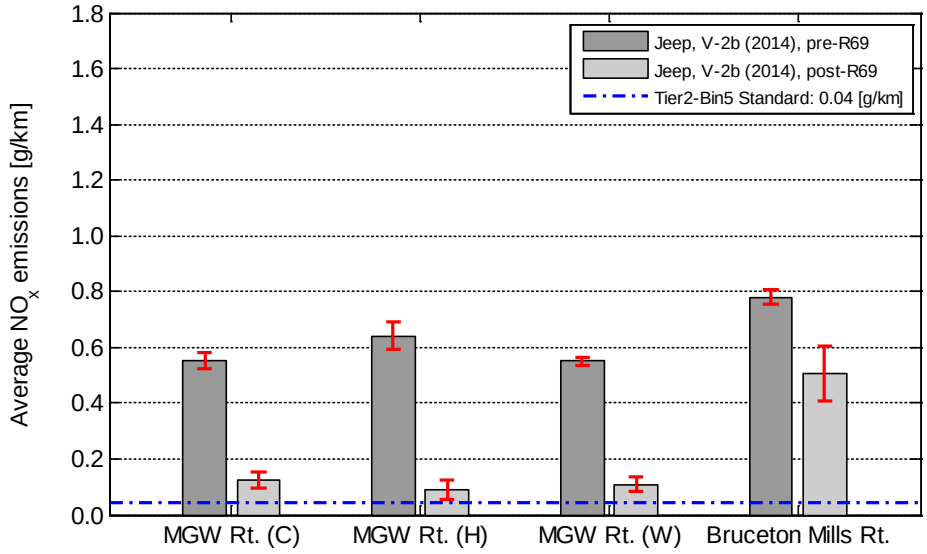

Figure 4.13: Comparison of average NO_x emissions of Jeep Grand Cherokee (Vehicle 2b), tested before and after recall R69 over two on-road driving routes compared to US-EPA Tier2-Bin5 (at full useful life) emissions standard; repeat test variation intervals are presented as ±1σ; MGW Rt. (C) - cold start; MGW Rt. (H) - run as hot start; MGW Rt. (W) - run as warm start after '*key-off*' and ~10min soak time.

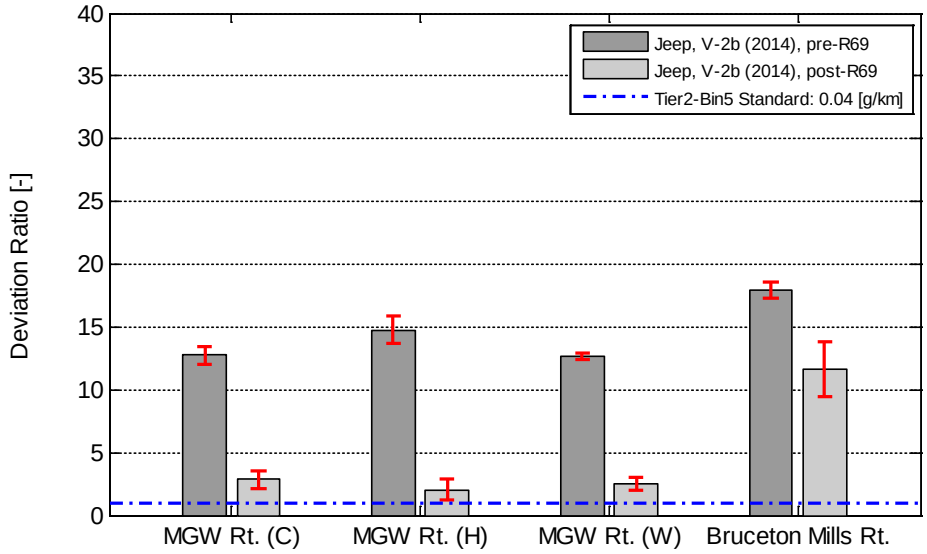

Figure 4.14: Comparison of average NO_x emissions of Jeep Grand Cherokee (Vehicle 2b), tested before and after recall R69 over two on-road driving routes expressed as deviation ratio; repeat test variation intervals are presented as ±1σ.

4.2 Comparison of Continuous Cycle and Route Emissions Rates

To provide clarity regarding the possible difference in emissions results collected from vehicle chassis dynamometer cycles and on-road routes, q-q plots are presented for engine load, vehicle speed and NO_x mass emissions rates. A q-q plot provides a means to visually assess if two data sets originate from populations with a common distribution. A quantile is defined as the fraction of the population that falls above or below a given threshold value. Thus, the 0.3 quantile is the point at which 30% of the population fall below that value and, conversely, 70 % fall above that value. Such comparison is appropriate for this analysis since data samples do not have to be of equivalent size. By plotting a x-y reference line, one can quickly assess if the two data sets come from populations with similar distribution, since the points would fall near this line. Departure from the x-y line correlates to increasingly dissimilar distributions of the two datasets. The regression line (i.e. red in the following plots) changes in format from dashed to solid at the 30-percentile, and once again at the 70-percentile level. The deviation of this regression line from the x-y degree reference line (i.e. blue) indicates increased quantile values for the abscissa. Deviation of the data from the linear regression model indicates a shift in quantile distribution from that of the linear model.

Figure 4.15 compares engine loads measured over the Bruceton Mills on-road route to those recorded from a US06 chassis dynamometer cycle for a MY 2014 Jeep Grand Cherokee (i.e. test vehicle 2b). This plot indicates that the majority of engine load points below 70% of maximum load points are higher in value for the Bruceton Mills route as compared to the US06 chassis dynamometer test cycle. The higher load points (i.e. above 70%) have a higher distribution for the US06 chassis dynamometer cycle. Figure 4.16 compares engine loads measured over the Morgantown on-road route to those recorded from a MGW chassis dynamometer cycle for the same vehicle. This figure indicates that for the majority of the data points (i.e. <70% of maximum load points) are equivalent for both on-road and chassis dynamometer tests. This is further supported by the slope of $\alpha = 0.0.9513$ as reported in Table 4.9, indicating slightly higher load for the chassis dynamometer (i.e. perfect agreement being a slope of $\alpha = 1.0$). Figure 4.17 indicates that the Bruceton Mills on-road route is characteristically higher in speed than the US06 chassis dynamometer cycle, while Figure 4.18 indicates that the MGW on-road route and MGW chassis dynamometer test cycle have very similar speed distribution. However, engine load from Figure 4.15 and Figure 4.16 are the more critical measure of performance similarity since exhaust

temperature, hence SCR catalytic activity, is more dependent upon engine load. Figure 4.19 and Figure 4.20 ultimately indicate that NO_x emissions for the on-road routes are predominantly higher than those measured over the chassis dynamometer test cycles. This is further supported by the increased slopes of $\alpha = 66.9634$ and $\alpha = 6.0676$ as reported in Table 4.9, indicating higher NO_x emissions for both on-road routes, Bruceton Mills and MGW, respectively, when compared to similar chassis dynamometer test cycles.

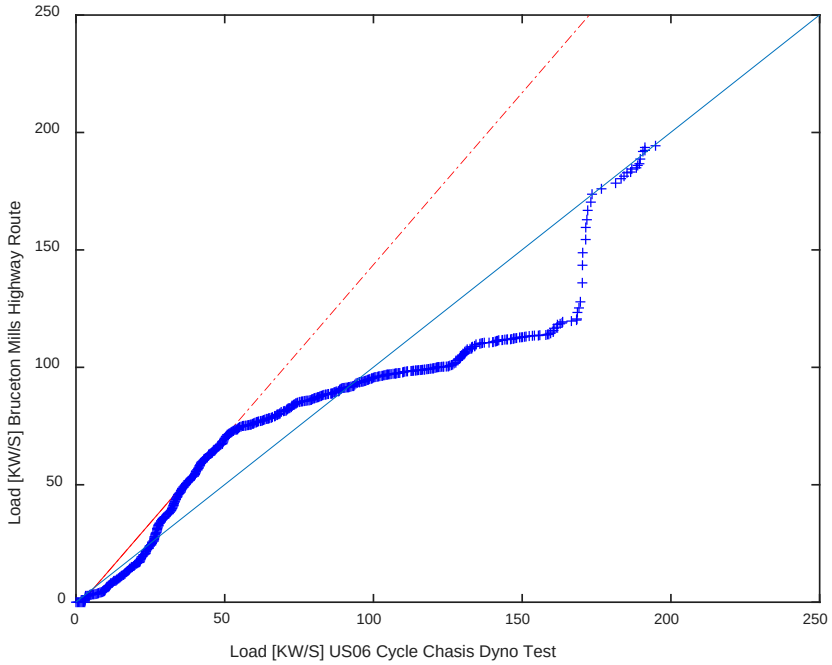

Figure 4.15: Comparison of engine load between the Bruceton Mills on-road route and the US06 chassis dynamometer cycle for Jeep Grand Cherokee MY'14.

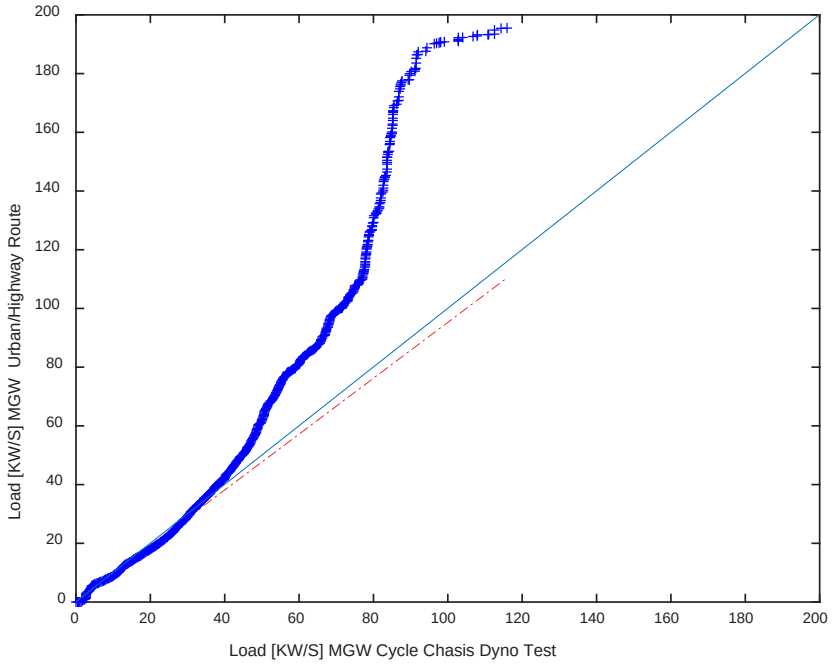

Figure 4.16: Comparison of engine load between the Morgantown on-road route and the MGW chassis dynamometer cycle for Jeep Grand Cherokee MY'14.

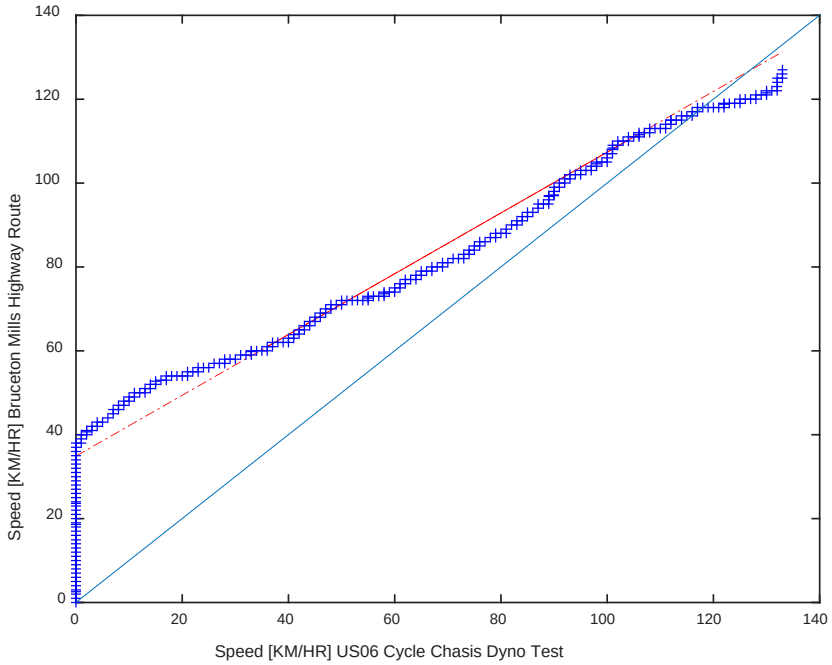

Figure 4.17: Comparison of vehicle speed between the Bruceton Mills on-road route and the US06 chassis dynamometer cycle for Jeep Grand Cherokee MY'14.

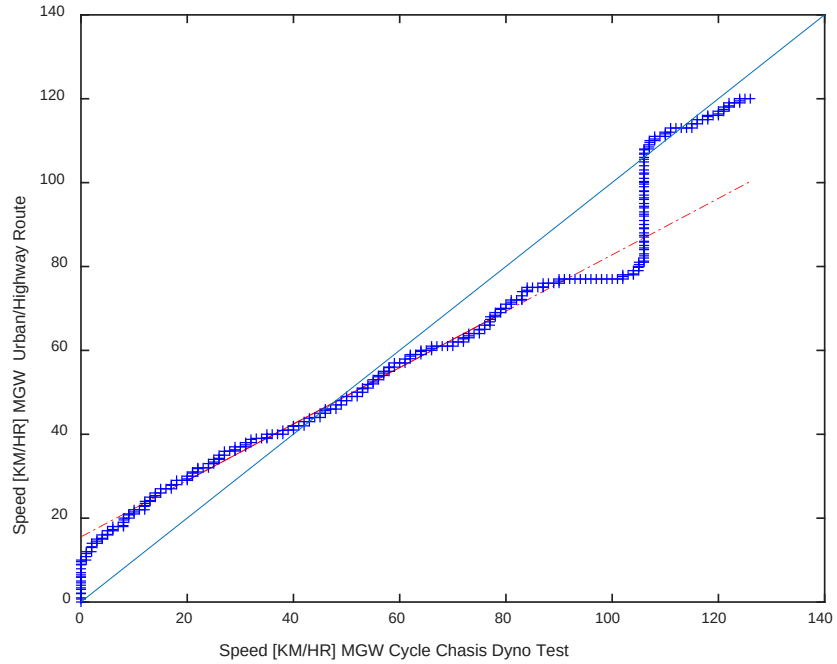

Figure 4.18: Comparison of vehicle speed between the Morgantown on-road route and the MGW chassis dynamometer cycle for Jeep Grand Cherokee MY'14.

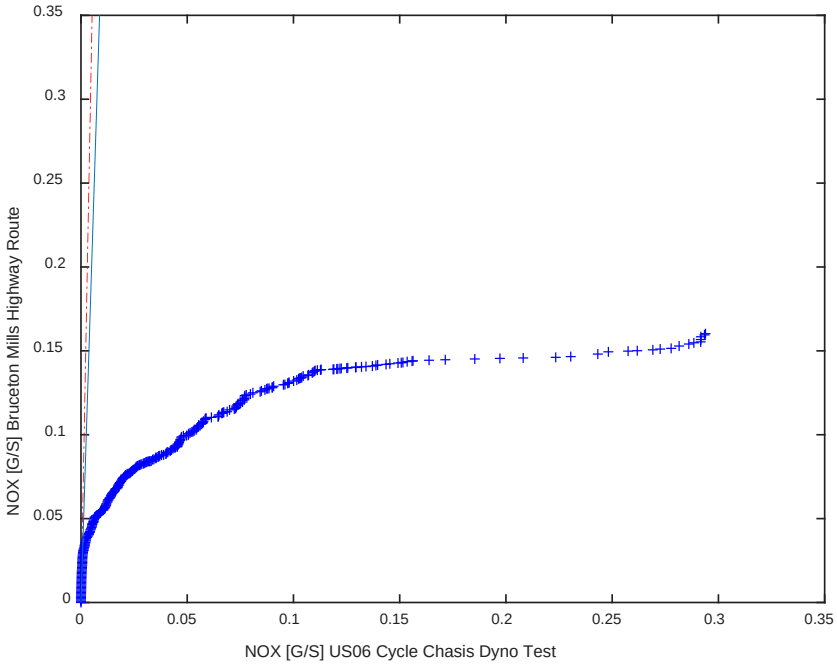

Figure 4.19: Comparison of NO_x emissions between the Bruceton Mills on-road route and the US06 chassis dynamometer cycle for Jeep Grand Cherokee MY'14.

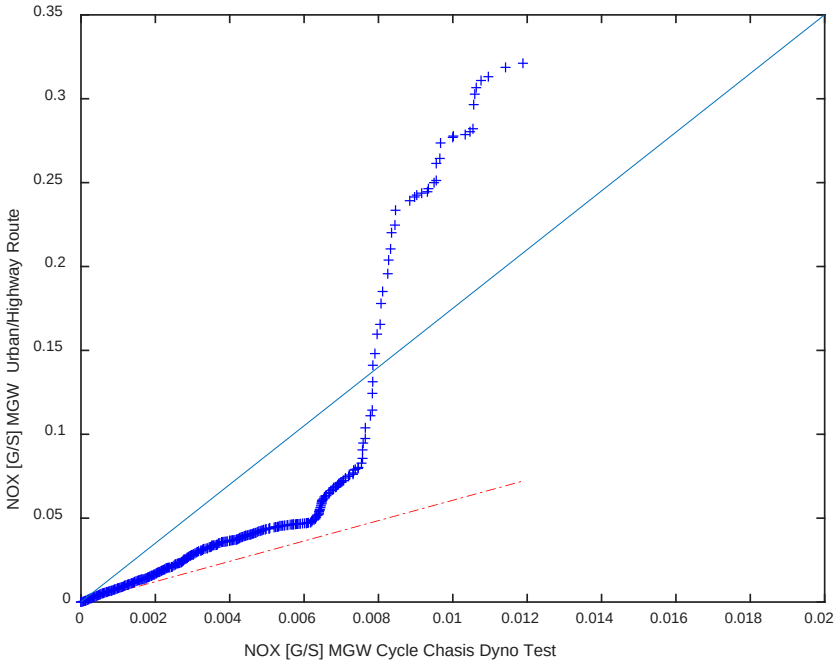

Figure 4.20: Comparison of NO_x emissions between the Morgantown on-road route and the MGW chassis dynamometer cycle for Jeep Grand Cherokee MY' 14.

Table 4.9: Q-Q plot parameters for mean and slope values for MY'14 Jeep Grand Cherokee (i.e. vehicle 2b)

	Engine load		NO_x mass rate		Vehicle speed	
Parameter	MGW road/chassis	Bruceton / US06	MGW road/chassis	Bruceton / US06	MGW road/chassis	Bruceton / US06
Mean (*Y/X*)	0.8121	0.747	4.7818	59.0063	1.0196	1.5922
Slope (*i.e. red line*)	0.9513	1.4651	6.0676	66.9634	0.6724	0.7246

Figure 4.21 and Figure 4.22 compare engine loads measured from on-road routes (i.e. Bruceton Mills and MGW route) to those recorded from chassis dynamometer cycles (US06 and MGW) for a MY 2015 Jeep Grand Cherokee (i.e. test vehicle 2). These plots indicate that recorded engine loads were predominantly higher for the on-road routes than for the vehicle chassis dynamometer cycles. This is further supported by the slopes of $\alpha = 0.9902$ and $\alpha = 1.3496$ as reported in Table 4.10 for the Bruceton-US06 and MGW-MGW analyses, respectively. Also similar to the 2014 Jeep Grand Cherokee analysis, Figure 4.23 indicates that the Bruceton on-road

routes is characteristically higher in speed than the US06 chassis dynamometer cycle, while Figure 4.24 indicates that the MGW on-road route and MGW chassis dynamometer test cycle have very similar speed distribution. As indicated previously, engine load is the more critical measure of performance similarity since exhaust temperature, hence SCR catalytic activity, is more dependent upon engine load. Figure 4.25 and Figure 4.26 indicate that NO_x emissions for the on-road routes are higher than those measured over the chassis dynamometer test cycles, which is further supported by the slope greater than unity that are reported in Table 4.10.

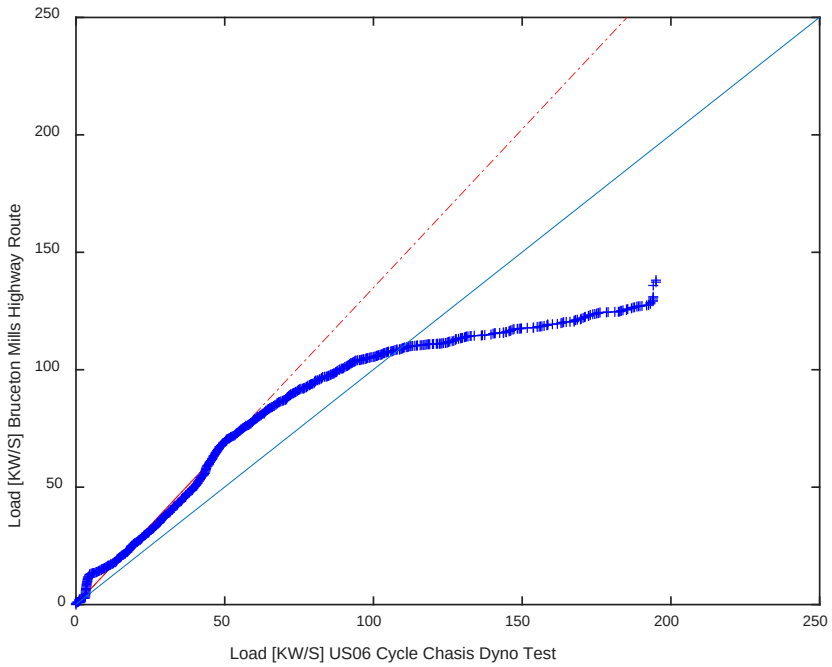

Figure 4.21: Comparison of engine load between the Bruceton Mills on-road route and the US06 chassis dynamometer cycle for Jeep Grand Cherokee MY'15.

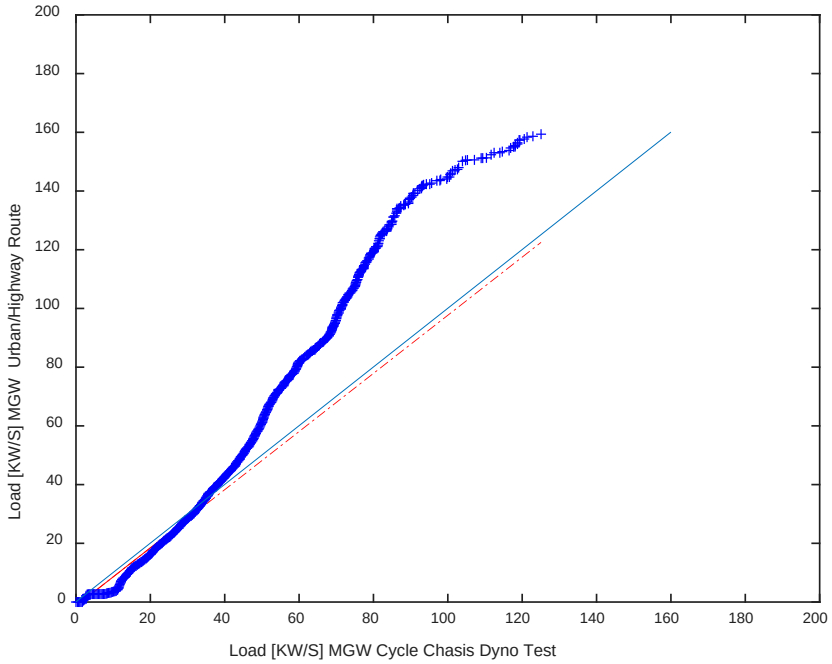

Figure 4.22: Comparison of engine load between the Morgantown on-road route and the MGW chassis dynamometer cycle for Jeep Grand Cherokee MY'15.

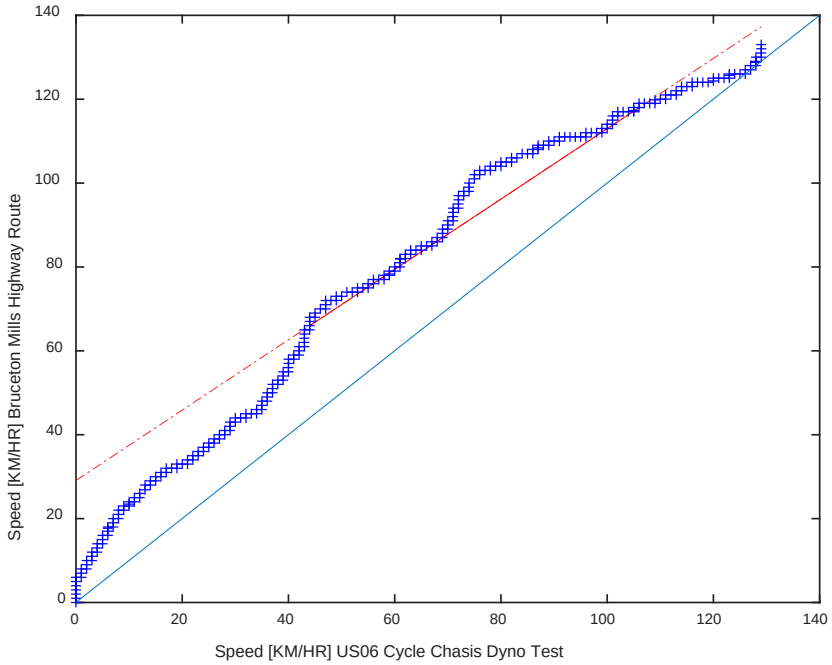

Figure 4.23: Comparison of vehicle speed between the Bruceton Mills on-road route and the US06 chassis dynamometer cycle for Jeep Grand Cherokee MY'15.

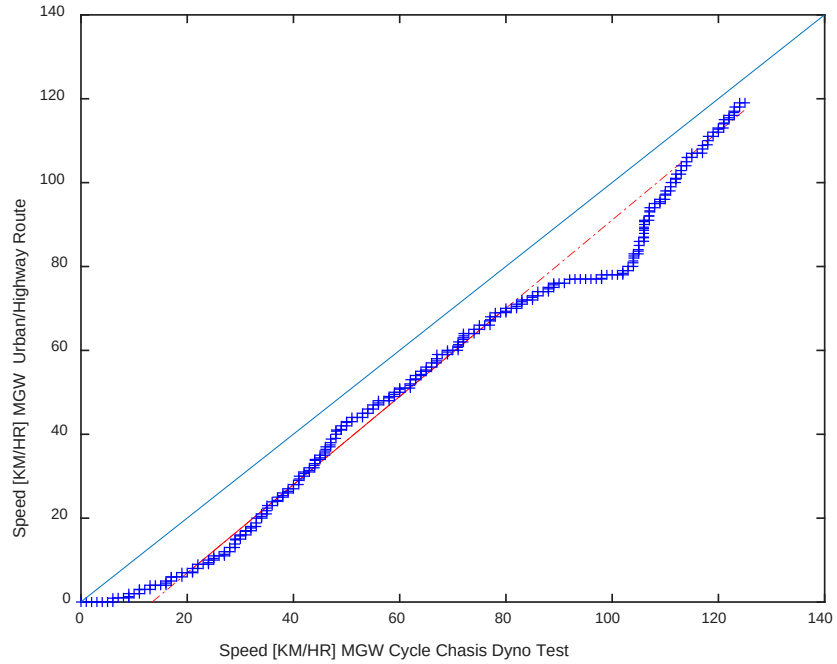

Figure 4.24: Comparison of vehicle speed between the Morgantown on-road route and the MGW chassis dynamometer cycle for Jeep Grand Cherokee MY'15.

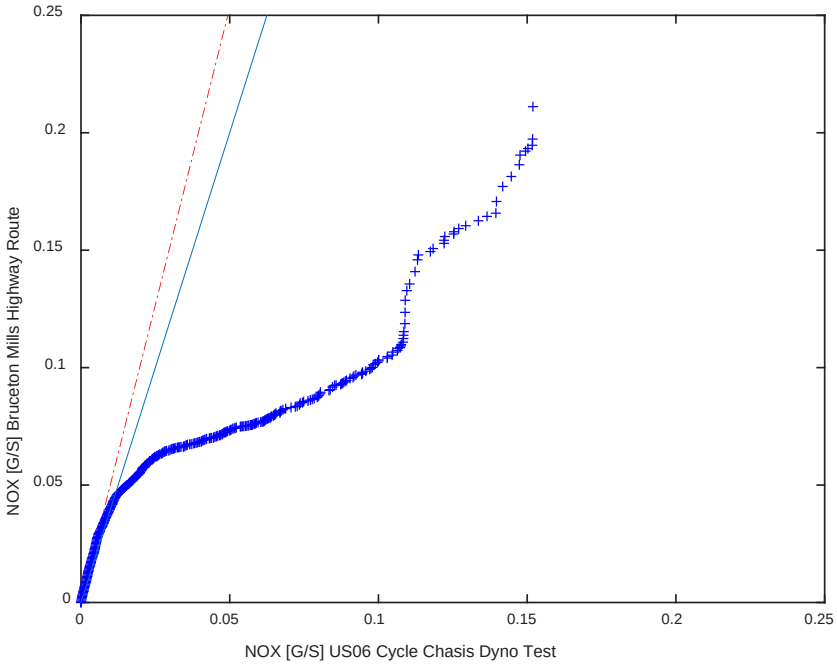

Figure 4.25 Comparison of NO_x emissions between the Bruceton Mills on-road route and the US06 chassis dynamometer cycle for Jeep Grand Cherokee MY'15.

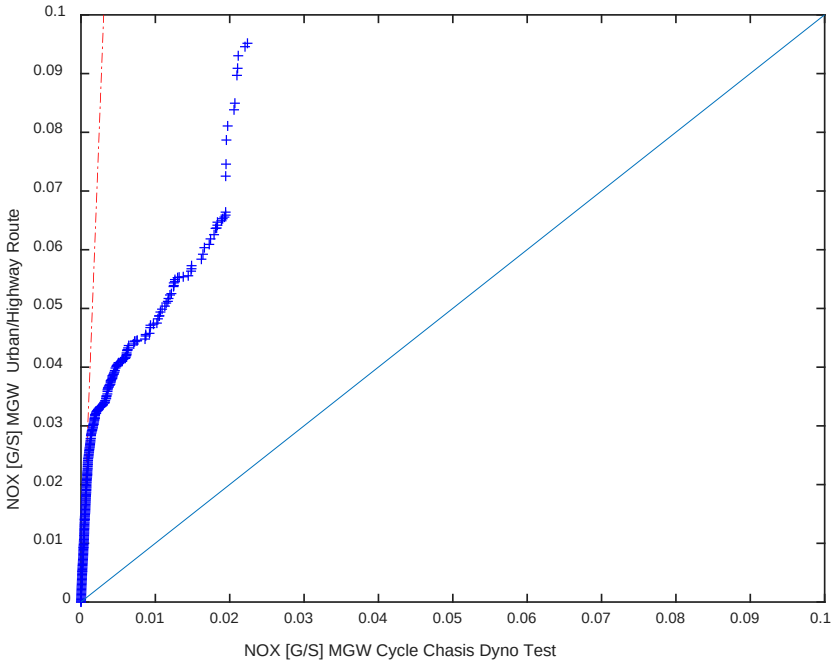

Figure 4.26: Comparison of NO_x emissions between the Morgantown on-road route and the MGW chassis dynamometer cycle for Jeep Grand Cherokee MY'15.

Table 4.10: Q-Q plot parameters for mean and slope values for MY'15 Jeep Grand Cherokee (i.e. vehicle 2)

	Engine load		**NO_x mass rate**		**Vehicle speed**	
Parameter	MGW road/chassis	Bruceton / US06	MGW road/chassis	Bruceton / US06	MGW road/chassis	Bruceton / US06
Mean (*Y/X*)	0.6492	1.078	18.5689	7.3219	0.6182	1.2433
Slope (*i.e. red line*)	0.9902	1.3496	32.7452	5.0615	1.0517	0.8387

In summary, when comparing continuous vehicle chassis dynamometer cycle and on-road route emissions rates, both the 2014 and 2015 Jeep Grand Cherokees (i.e. test vehicles 2 and 2b) produced higher emissions for the on-road routes. Moreover, these elevated NO_x emissions were coincident with higher engine loads, which would typically produce thermodynamic conditions that would be more conducive to higher NO_x conversion rates when implementing SCR NO_x emissions control technology. This conclusion was particularly curious for the MGW route and cycle, since actual route operation is simulated in the controlled laboratory environment, and data suggested very similar trends with respect to engine load.

4.3 Characterization of Hardware and ECU Software Impacts on Emissions

After initial on-road testing was performed on a MY 2014 Jeep Grand Cherokee (i.e. test vehicle 2b), the owner of that vehicle was notified of FCA Emissions Recall R69 [25], which required replacement of DEF injector, SCR catalyst and ECU re-programming. Upon successful completion of the recall, the vehicle was again recruited to complete follow-up testing (both vehicle chassis dynamometer and on-road testing).

Figure 4.27 provides continuous NO_x emissions rates measured from the MY 2014 Jeep Grand Cherokee (i.e. vehicle 2b) with pre- and post-recall (R69) configurations while being operated over the MGW route. Average deviation ratios over the in-use MGW route (i.e. rural/urban) were observed between 12 and 28 for *cold* and *warm-start*, respectively, for the pre-recall configuration, compared to 2.1 to 2.9 for a post-recall tests.

Figure 4.28 provides continuous NO_x emissions rates measured from the same test vehicle with pre- and post-recall (R69) configurations while being operated over the Bruceton Mills route. Average deviation ratios over the in-use Bruceton Mills route (i.e. highway) were observed as 17.7 for the pre-recall, compared to 11.6 for the post-recall tests. It shall be noted that the on-road routes (i.e. MGW Rt. and Bruceton Mills Rt.) were slightly modified after completion of the pre-recall testing because the starting point of the test route was relocated to accommodate commissioning of the new CAFEE testing facility. As a result, total route distances changed (pre/post) from 36km to 40km for the MGW Rt. and 100km to 80km for the Bruceton Mills Rt. for the test program. This had little effect on vehicle activity across the MGW route and reduced non-highway operation for the Bruceton Mills route. Overall impact on vehicle operation and subsequent integrated emissions was minimal.

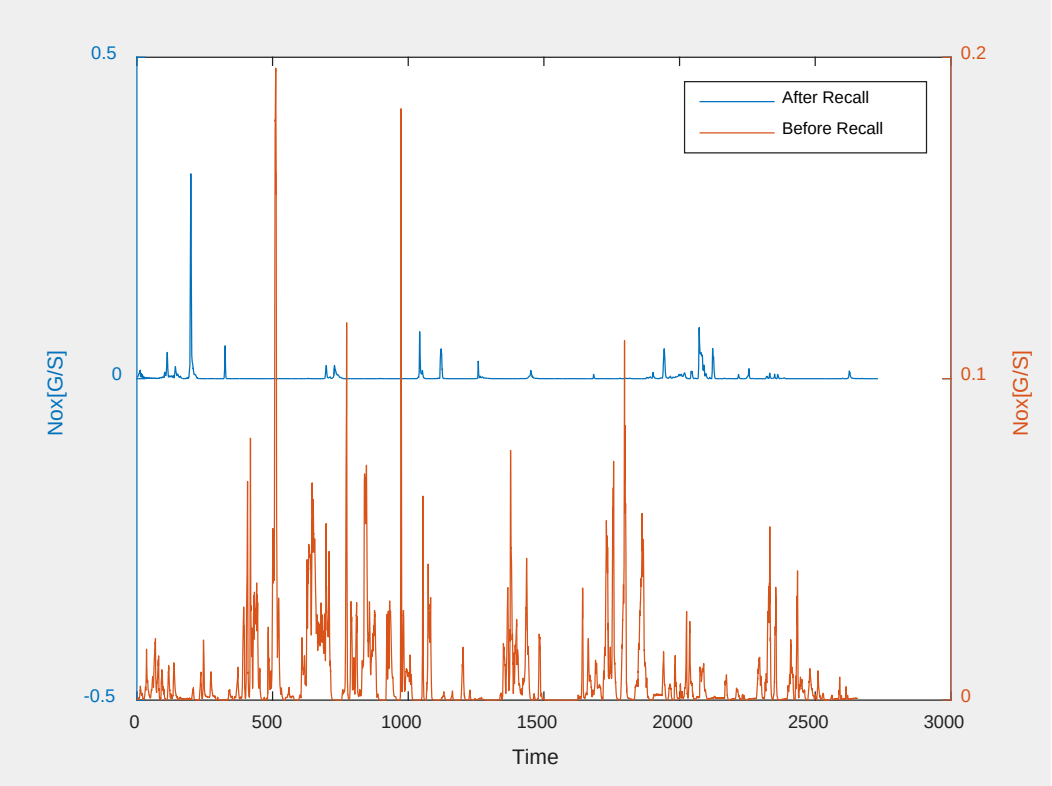

Figure 4.27: Comparison of continuous NO_x emissions rates in [g/s] from a MY 2014 Jeep Grand Cherokee before and after the R69 recall over the Morgantown route.

Due to the change in emissions performance of the MY 2014 Jeep Grand Cherokee following the R69 recall, and the discovery of similar notices, such as Service Bulletin 18-064-15 [26] that involved replacement of components of the emissions control system, the CAFEE conducted further investigation into the recall and its subsequent impact on emissions characteristics and vehicle performance. In April 2016, Chrysler issued Emissions Recall R69 for the SCR catalyst. Per the recall [25], the following part numbers could be required for vehicles:

Table 4.11: Components included in R69 emissions recall.

Part Number	Description
68243268AB	Converter, SCR Catalyst (WK 4WD only)
68243267AB	Converter, SCR Catalyst (WK 2WD only)
68263789AB	Converter, SCR Catalyst (DS vehicles with 140 inch wheelbase)
68263790AB	Converter, SCR Catalyst (DS vehicles with 149 inch wheelbase)
68160679AB	Gasket, SCR Catalyst
68234976AA	Gasket, Diesel Exhaust Fluid (DEF) Injector
06105052AA	Bolt, SCR Catalyst Fastener (Qty. 3)
06506619AA	Nut, SCR Catalyst Fastener (Qty. 3)

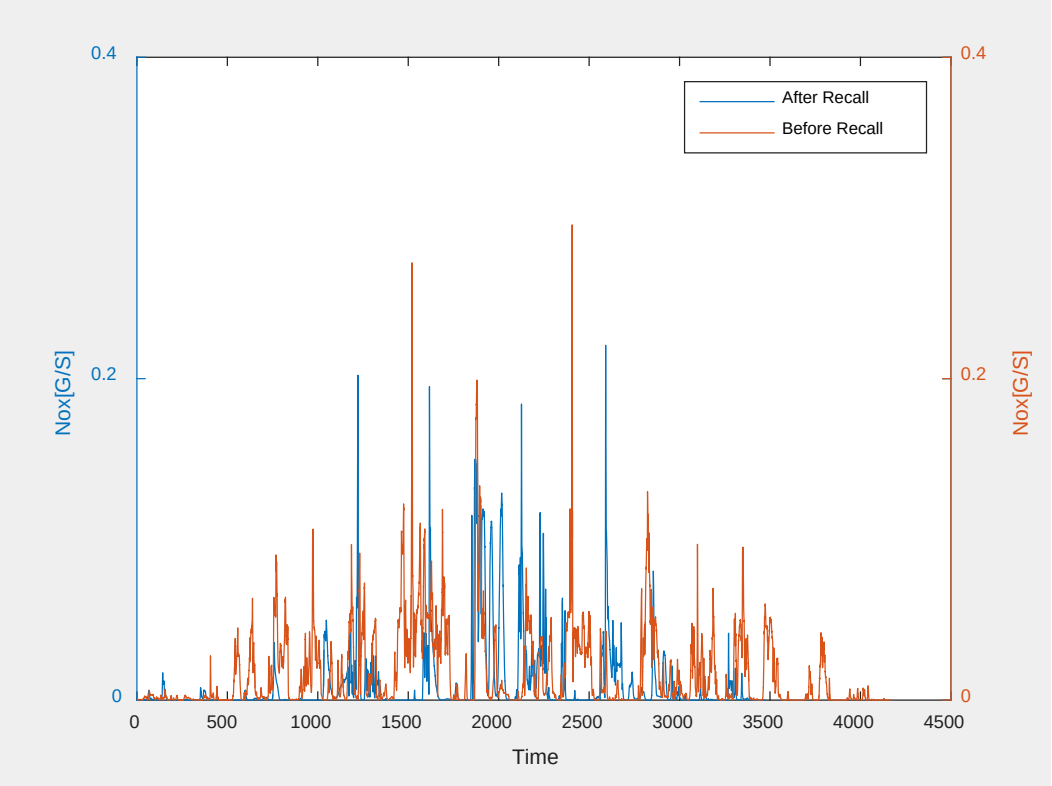

Figure 4.28: Comparison of continuous NO_x emissions rates in [g/s] from a MY 2014 Jeep Grand Cherokee before and after the R69 recall over the Bruceton Mills route.

As part of the R69 recall process, the following '*non-hardware*' related procedure was required. Use of the following procedure to perform the SCR catalyst reset (i.e. taken from [25]).

a. Connect the wiTECH scan tool and start a session.
b. From the "PCM View" screen, click on the "Miscellaneous Functions" tab.
c. Perform the SCR System Catalyst Reset function.
d. Using the wiTECH scan tool, clear all Diagnostic Trouble Codes (DTCs).

In order to perform this service function, an AE Tools Mopar MicroPOD II (https://www.aetools.us/products/mopar-micropod-ii/) was purchased. The system was supplied with added functionality provided by separate Tech Authority Software Subscription that provided CAFEE access to Module Re-Flash Programming. As such, physical ECU replacement could be made for the test vehicles to '*simulate*' pre- and post-recall performance. However, it is noted that parameter value transfers did occur during the synchronization (i.e. '*marriage*') of ECU to vehicle procedure. As such, CAFEE cannot confirm that the resultant ECU state was truly equivalent to that of an actual pre- or post-recall unit once the AE tool was utilized.

The CAFEE secured components necessary to conduct *A-B comparison testing* of two vehicles to elucidate the impact on vehicle performance. For this portion of the project, the following test vehicles were utilized:

a. Jeep Grand Cherokee, MY2014 (i.e. test vehicle 2b)
b. Ram 1500, MY 2014 (i.e. test vehicle 1d)

The MY 2014 Jeep Grand Cherokee had the R69 recall performed by an FCA authorized service center (Chrysler-Jeep dealership). As such, CAFEE secured pre-recall DEF injector, SCR catalyst and ECU from salvage vehicles that were subject to the recall, but had not participated in the recall process. Once the ECU was synchronized to be compatible with the vehicle, the Jeep Grand Cherokee could be configured arbitrarily with hardware and control software (i.e. via ECU replacement) that '*simulated*' pre- and post-recall states.

The MY 2014 Ram 1500 was delivered to a Chrysler dealership for participation in the formal R69 recall. Prior to the recall, pre-recall DEF injector and SCR catalyst were removed and replaced with units purchased from a Chrysler dealership. A secondary ECU was purchased from a salvage vehicle and synchronized to the test vehicle using the AE tools system, prior to presenting the vehicle for recall. As such, the original pre-recall ECU and hardware were retained for this vehicle so that it could similarly be configured arbitrarily with hardware and control software (i.e. via ECU replacement) that '*simulated*' pre- and post-recall states.

With the above functionality, both test vehicles were subjected to the following test configurations:

1. Pre-recall hardware and pre-recall software
2. Pre-recall hardware and post-recall software
3. Post-recall hardware and pre-recall software
4. Post-recall hardware and post-recall software

It shall be noted, that configurations 2 and 3, above, were research combinations that would not be developed or provided by FCA as a compliant solution. Rather, these combinations were tested to elucidate performance changes resultant of the respective (hardware or software) recall.

Figure 4.29 provides continuous NO_x emission rates for the MY 2014 Jeep Grand Cherokee over the MGW in-use route and the MGW chassis dynamometer cycle after the R69 recall was

performed. Although integrated NO_x emissions were lower for the laboratory-based chassis dynamometer cycles, the on-road test route operation still exhibited elevated NO_x emissions.

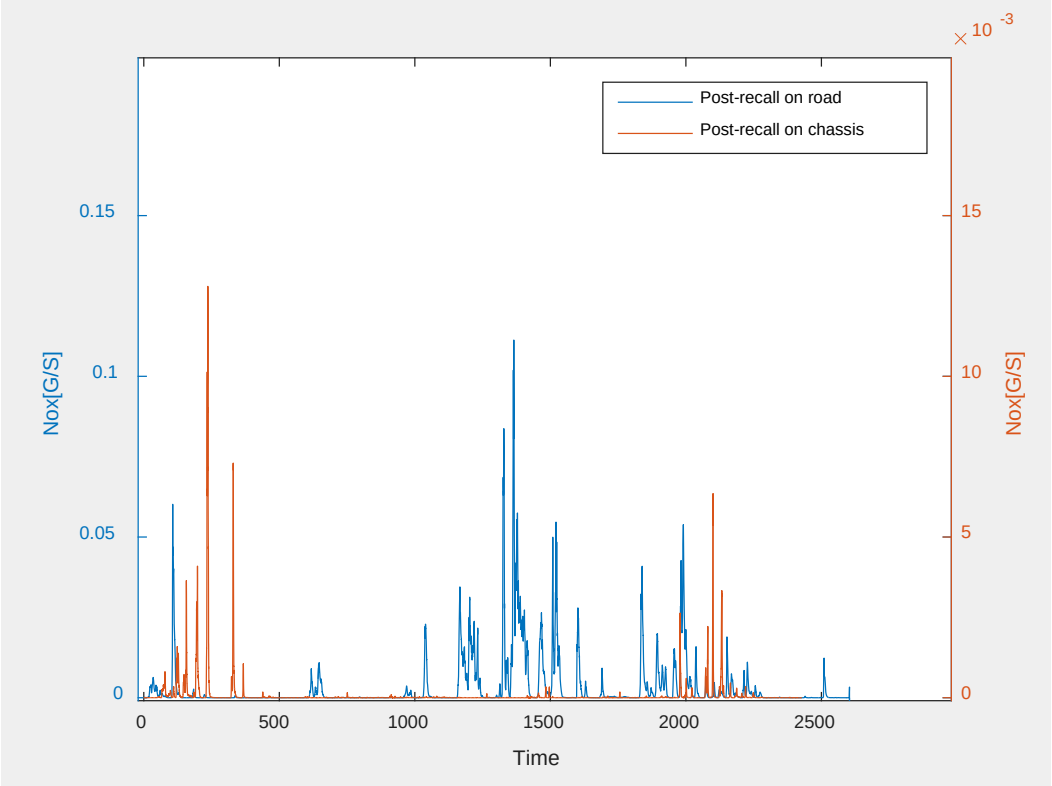

Figure 4.29: Comparison of NO_x emissions rates in [g/s] from the 2014 Jeep Grand Cherokee after R69 recall between chassis dynamometer and on-road tests (i.e. MGW cycle vs. MGW route).

Figure 4.30 and Figure 4.31 provide continuous NO_x emissions rates for the MY 2014 Ram 1500 over the MGW in-use route and the MGW chassis dynamometer cycle before and after the R69 recall was performed, respectively.

Consistent with those results from the 2014 Jeep Grand Cherokee that underwent the R69 recall, the 2014 Ram 1500 test vehicle continued to produce elevated NO_x emissions during on-road operation. However, the 2014 Ram 1500 test vehicle continued to produce NO_x emission at similar levels after the recall, in contrast to the improved on-road performance of the 2014 Jeep Grand Cherokee.

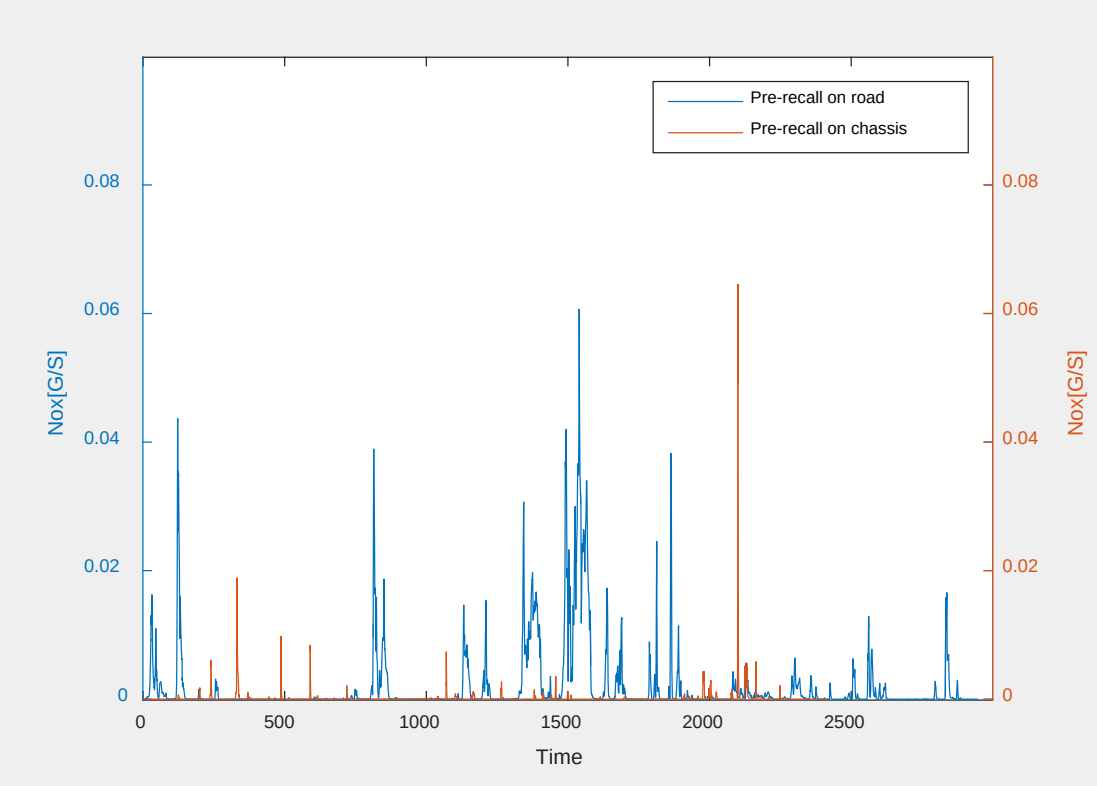

Figure 4.30: Comparison of NO_x emissions rates in [g/s] from the 2015 Ram 1500 prior to R69 recall between chassis dynamometer and on-road tests (i.e. MGW cycle vs. MGW route).

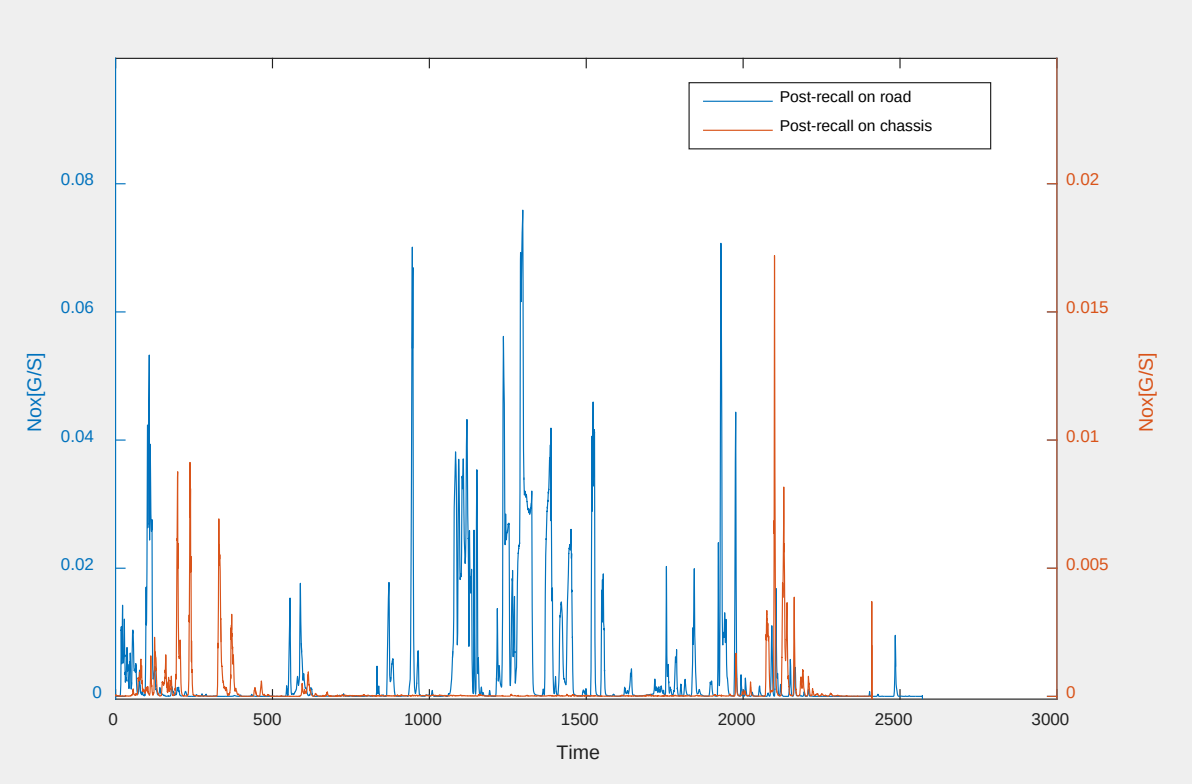

Figure 4.31: Comparison of NO_x emissions rates in [g/s] from the 2015 Ram 1500 after R69 recall between chassis dynamometer and on-road tests (i.e. MGW cycle vs. MGW route).

Figure 4.32 presents average NO_x emissions factors from a MY 2014 Jeep Grand Cherokee (i.e. test vehicle 2b) over on-road test routes for the software (ECU) and hardware (injector and SCR catalyst) revisions characterized by pre- and post-recall (R69) state. Figure 4.33 presents the same data in terms of deviation ratios, rather than distance-specific NO_x emissions factors. For MGW routes, the full recall (post-R69) produced the lowest NO_x emissions. The combinations of pre-recall ECU/post-recall hardware and post-recall ECU/pre-recall hardware produced the next lowest values. For the combinations of pre-recall ECU/pre-recall hardware and full pre-recall (pre-R69), NO_x deviation ratios in excess of 10 (i.e. over 10 times the emissions certification standard) were recorded for the on-road MGW routes. Although the distribution of emissions results trend in an increasing fashion across these combination software/hardware revisions, it is not conclusive as to which components (software or hardware) influence NO_x production the most. This may be resultant of arbitrary combinations that were not intended to be integrated into the same system, or my simply be a product of ECU updating and parameter value transfers that concluded in

software revisions not truly representative of a pre-recall state. However, it is apparent that improved on-road NO_x emissions control was exhibited by the full R69 recall when compared to the original pre-R69 configuration. Nevertheless, Figure 4.29 indicates that on-road emissions were still very different from chassis dynamometer test results, even for the very similar operating conditions of the MGW route and MGW cycle. In addition, Table 4.12 and Table 4.13 summarize the average NO_x emissions factors and respective deviation ratios for the four test combinations.

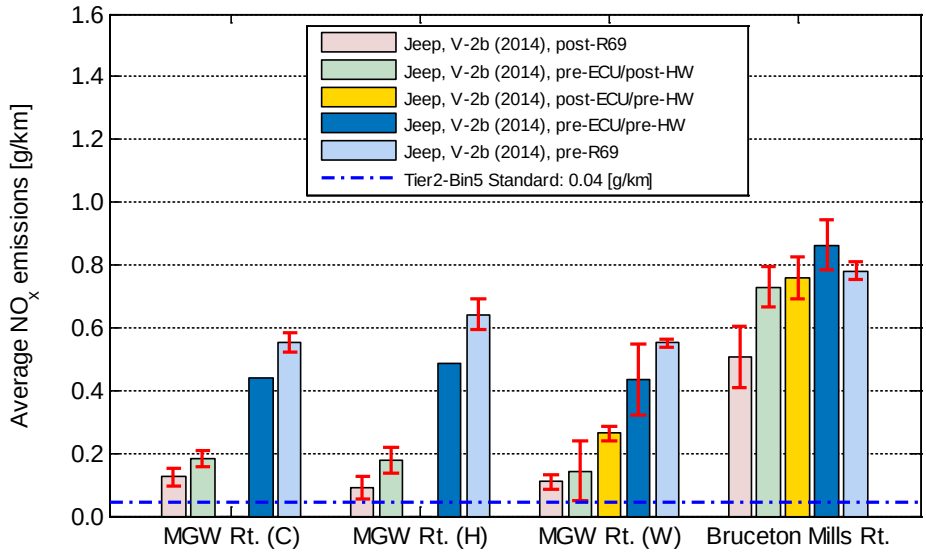

Figure 4.32: Average NOx emissions of Jeep Grand Cherokee (Vehicle 2b) test vehicle over two on-road driving routes and four different software/hardware configurations, compared to US-EPA Tier2-Bin5 (at full useful life) emissions standard; repeat test variation intervals are presented as ±1σ; MGW Rt. (C) - cold start; MGW Rt. (H) - run as hot start; MGW Rt. (W) - run as warm start after '*key-off*' and ~10min soak time.

Table 4.12: Average NO_x emissions in [g/km] for Jeep Grand Cherokee (Vehicle 2b) test vehicle over two on-road driving routes and four different software/hardware configurations; σ is standard deviation over consecutive test runs.

Cycle		Post-Recall	Pre-ECU /Post-HW	Pre-ECU /Post-HW	Pre-ECU /Post-HW	Pre-Recall
MGW Rt. (Cold)	**μ**	**0.1244**	**0.1845**	-	**0.4379**	**0.5539**
	σ	*0.0294*	*0.0259*	-	-	*0.0302*
MGW Rt. (Hot)	**μ**	**0.0894**	**0.1781**	-	**0.4882**	**0.6417**
	σ	*0.0348*	*0.0429*	-	-	*0.0483*
MGW Rt. (Warm)	**μ**	**0.1094**	**0.1438**	**0.2632**	**0.4329**	**0.5506**
	σ	*0.0238*	*0.0933*	*0.0215*	*0.1128*	*0.0132*
Bruceton Mills Rt.	**μ**	**0.5063**	**0.7293**	**0.7589**	**0.8633**	**0.7810**
	σ	*0.0970*	*0.0648*	*0.0680*	*0.0784*	*0.0276*

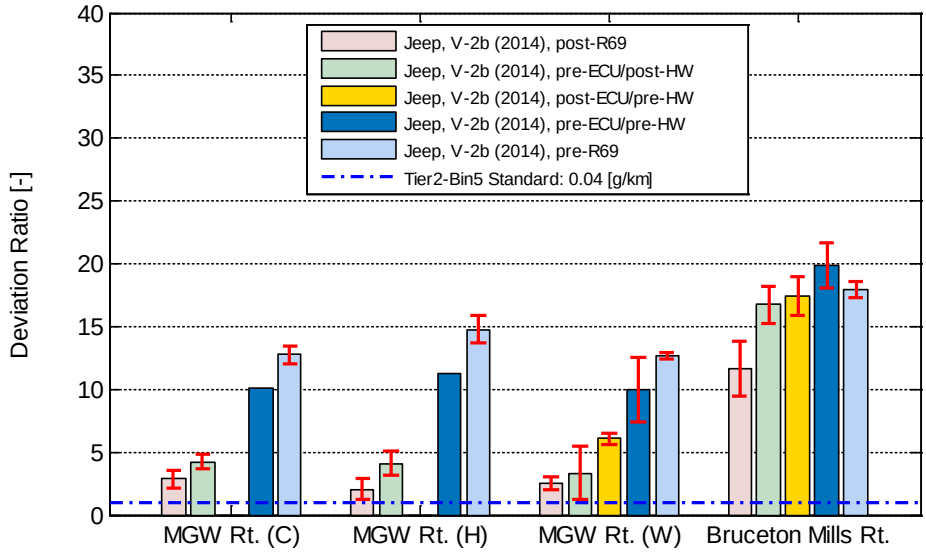

Figure 4.33: Average NO_x emissions of Jeep Grand Cherokee (Vehicle 2b) test vehicle over two on-road driving routes and four different software/hardware configurations, expressed as deviation ratio; repeat test variation intervals are presented as ±1σ.

Table 4.13: Average NO_x emissions in [g/km] for Jeep Grand Cherokee (Vehicle 2b) test vehicle over two on-road driving routes and four different software/hardware configurations, expressed as deviation ratio; σ is standard deviation over consecutive test runs.

Cycle		Post-Recall	Pre-ECU /Post-HW	Pre-ECU /Post-HW	Pre-ECU /Post-HW	Pre-Recall
MGW Rt. (Cold)	**μ**	**2.86**	**4.24**	-	**10.07**	**12.73**
	σ	*0.68*	*0.60*	-	-	*0.69*
MGW Rt. (Hot)	**μ**	**2.06**	**4.10**	-	**11.22**	**14.75**
	σ	*0.80*	*0.99*	-	-	*1.11*
MGW Rt. (Warm)	**μ**	**2.51**	**3.31**	**6.05**	**9.95**	**12.66**
	σ	*0.55*	*2.14*	*0.49*	*2.59*	*0.30*
Bruceton Mills Rt.	**μ**	**11.64**	**16.77**	**17.45**	**19.85**	**17.95**
	σ	*2.23*	*1.49*	*1.56*	*1.80*	*0.63*

5 CONCLUSIONS

The primary objective of the study was to characterize the performance of NO_x after-treatment conversion efficiencies of recruited test vehicles when they are being tested in the laboratory (i.e. chassis dynamometer) as well as over-the-road (i.e. on-road). These results were then used to identify those parameters that most affected the vehicles' emissions performance. For all tests, gaseous exhaust emissions, including oxides of nitrogen (NO_x), nitrogen oxide (NO), carbon monoxide (CO), carbon dioxide (CO_2), and total hydrocarbons (THC) were measured on a continuous basis utilizing a portable emissions measurement system (PEMS) from Horiba®. Additionally, total particle number concentrations were quantified using a real-time particle sensor from Pegasor (PPS).

The test vehicles were all equipped with the 3.0L EcoDiesel engine, and featuring selective catalytic reduction (SCR) NO_x after-treatment technology. As such, the NO_x control of these vehicles is ultimately dependent upon the ability to initiate catalytic activity. Results collected from tests conducted on the vehicle chassis dynamometer suggested that all 5 vehicles were emissions-compliant, enabling the conclusion that all were representative test articles. It shall be noted that this does not provide complete assurance that off-cycle emissions performance during other operating conditions was not the result of negotiated AECDs or prior mal-maintenance or system tampering. When most of the test vehicles were tested over-the-road, elevated NO_x emissions were recorded (i.e. increased deviation ratios from the US-EPA Tier2 Bin5 standard), although data suggest that similar operating conditions were being encountered by the test vehicles as during chassis dynamometer testing. This result remained consistent, even for vehicle routes that were used to generate '*simulated*' chassis dynamometer cycles that mimicked real-world driving patterns. The MY 2015 Jeep Grand Cherokee vehicle exhibited lower NO_x deviation ratios, while MY 2014 Ram 1500 vehicles demonstrated the highest NO_x deviation results.

Two of the vehicles (MY 2014 Jeep Grand Cherokee and MY 2014 Ram 1500) from the test population were selected for more in-depth analyses since they were subject to the FCA R69 emissions recall. These vehicles were configured with hardware (i.e. DEF injector and SCR catalyst) and ECU software revisions in order to '*simulate*' pre- and post-recall emissions performance. In addition, components were combined in an attempt to further clarify how these recalled components independently affected vehicle emissions. The MY 2014 Jeep was not

originally tested on the chassis dynamometer in the pre-recall state. However, its post recall performance was aligned with those emissions results to which the engine family was certified. On-road NO_x deviation ratios for this vehicle for pre-recall operation averaged in the 18-20 range, whereas post recall ratios were recorded to be in the 2-4 range. However, combinations of hardware components (i.e. DEF injector and SCR catalyst) and software control (ECU) did not provide results that would substantiate a conclusion that hardware was the clear reason for poor over-the-road emissions performance. A MY 2014 Ram 1500 was tested for both pre- and post-recall configurations in the laboratory (i.e. chassis dynamometer) as well as over-the-road (i.e. on-road). Laboratory tests for both configurations produced emissions that were compliant with those against which the vehicle was certified. However, on-road test results did not provide conclusive evidence that the recall improved on-road performance. The authors note that some of the combinations used in the attempt to isolate the emissions impact of hardware and software were not representative of any vehicle configuration that was produced by FCA.

6 REFERENCES

1 "US EPA, Fuel Economy Guide Web Site," Available at http://www.fueleconomy.gov, Last updated: March 17, (2014).

2 COMMISSION REGULATION (EU) No 582/2011, Official Journal of the European Union, May 25th, (2011).

3 COMMISSION REGULATION (EU) No 459/2012, Official Journal of the European Union, May 29th, (2012).

4 "US EPA, Emission Standards Reference Guide: Vehicle Weight Classifications," Available at http://www.epa.gov/otaq/standards/weights.htm, Last updated: November 14, (2012).

5 "Control of Air Pollution From New Motor Vehicles: Tier 2 Motor Vehicle Emissions Standards and Gasoline Sulfur Control Requirements; Final Rule," US Environmental Protection Agency, Federal Register Vol. 65, No. 28, pp. 6698 - 6870, February 10th, (2000).

6 Weiss, M., Bonnel, P., Hummel, R., and Steininger, N., "A complementary emissions test for light-duty vehicles: Assessing the technical feasibility of candidate procedures," JRC Scientific and Technical Reports, EUR 25572 EN, (2013).

7 Ericsson, E., "Variability in urban driving patterns," Transportation Research Part D, Vol. 5, pp. 337-354, (2000).

8 Delgado-Neira, O.F., "Driving Cycle Properties and their Influence on Fuel Consumption and Emissions," Ph.D. Dissertation, West Virginia University, (2012).

9 Delgado, O.F., Clark, N.N., and Thompson, G.J. "Method for translation of in-use fuel consumption and NO_x emissions between different heavy-duty vehicle routes," Proceedings of the ASME 2011 Internal Combustion Engine Division Fall Technical Conference, Paper No. ICEF2011-60108, Morgantown, WV, October 2nd - 5th, (2011).

10 "The Federal Test Procedure & Unified Cycle," California Air Resources Board's Emissions Inventory Series, Volume 1, Issue 9, (*not dated*).

11 Praveen, R. B., "Measurement of Road Grade for In-use Emissions Testing Assessment," Master's Thesis, West Virginia University, December, (2012).

12 "Control of Emissions from New and In-Use Highway Vehicles and Engines," US Environmental Protection Agency, Federal Register, Title 40, Vol. 86, Subpart B, §86.158-08(c), pp. 555, (2008).

13 California Air Resources Board, "Enhanced Supplemental Federal Test Procedures Rulemaking - SFTP II," Meeting Presentation, Sacramento, (2010).

14 Horiba Ltd., "On Board Emission Measurement System OBS-2200 - Instruction Manual," March, (2009).

15 Khalek, I., "PM-PEMS Measurement Allowance Determination," Final Report, SWRI, Project 03.14936.12, June, (2010).

16 Bonnel, P., Carriero, M., Forni, F., Alessandrini, S., Montigny, F., Demircioglu, H., and Giechaskiel, B., "EU-PEMS PM Evaluation Program - First Report," JRC Scientific and Technical Reports, EUR 24543 EN, (2010).

17 Mamakos, A., Carriero, M., Bonnel, P., Demircioglu, H., Douglas, K., Alessandrini, S., Forni, F., Montigny, F., and Lesueur, D., "EU-PEMS PM Evaluation Program - Second Report - Study of Post DPF PM/PN," JRC Scientific and Technical Reports, EUR 24793 EN, (2011).

18 Mamakos, A., Carriero, M., Bonnel, P., Demircioglu, H., Douglas, K., Alessandrini, S., Forni, F., Montigny, F., and Lesueur, D., "EU-PEMS PM Evaluation Program - Third Report - Further Study on Post DPF PM/PN Emissions," JRC Scientific and Technical Reports, EUR 24883 EN, (2011).

19 Giechaskiel, B., Carriero, M., Bonnel, P., Schindler, W., Scheder, D., Bassoli, C., and Niemela, V., "Feasibility of Particulate Mass and Number Measurement with Portable Emission Measurement Systems (PEMS) for In-Use Testing," SAE Technical Paper Number 2011-24-0199, (2011).

20 Wei, Q., Rooeny, R., "The On-Board PM Mass Calibration for the Real-Time PM Mass Measurement," SAE Technical Paper Number 2010-01-1283, (2010).

21 Pegasor Ltd., "PPS Brochure," www.pegasor.fi, Finland, Accessed June, (2011).

22 Tikkanen, J., and Ntziachristos, L., "Pegasor Particle Sensor (PPS) - Potential solution for On-Board Diagnosis of Particle Filter Operation - First Results and Development Potential," 4th Biennial Conference – Emissions Solutions in Transportation, Ann Arbor, MI, October 5-8, (2009).

23 Besch, M.C., Thiruvengadam, A., Kappanna, H.K., Cozzolini, A., Carder, D.K., and Gautam, M., "Assessment of Novel In-Line Particulate Matter Sensor with Respect to OBD and Emissions Control Applications," Proceedings of the ASME 2011 ICE Division Fall Technical Conference, ICEF2011-60142, Paper Accepted for Publication, (2011).

24 "Engineering Statistics Handbook," Available at http://www.itl.nist.gov/div898/handbook/eda/section3/eda33o.htm.

25 Fiat Chrysler Automobiles, "Emissions Recall R69 Selective Catalytic Reduction Catalyst," https://www.chrysler.com/universal/webselfservice/pdf/R69.pdf.

26 Fiat Chrysler Automobiles, "Service Bulletin 18-064-15," September 24, 2015 http://www.wk2jeeps.com/tsb/tsb_wk2_1806415.pdf

27 Ntziachristos, L., Amanatidis, S., Rostedt, A., Janka, K., and Tikkanen, J., "Optimization of the Pegasor Particle Sensor for Automotive Exhaust Measurements," 23rd CRC Real World Emissions Workshop, San Diego, CA, April 7th-10th, (2013).

28 Ntziachristos, L., Amanatidis, S., Rostedt, A., Keskinen, K., Janka, K., and Tikkanen, J., "Calibration and performance of a novel particle sensor for automotive application," EAC - 2012, European Aerosol Conference, Granada, Spain, September 2nd-7th, (2012).

29 United Nations, ECE/TRANS/WP.29/GRPE/2012, Regulation No.49, Annex 4, Appendix 8, "Particle Number Emissions Measurement Equipment," (2012).

30 Tikkanen, J., Janka, K., Rostedt, A., Röbel, M., Amanatidis, S., and Ntziachristos, L., "Dilution Artifacts. A Significant Source of Error from Absolute Concentration and Possibly Difficult to Reproduce. PMP vs. Raw Exhaust," 17th ETH Conference on Combustion Generated Nanoparticles, Zurich, Switzerland, June 23rd - 26th, (2013).

31 Code of Federal Regulations, Title 40, Part 1065, "Engine-Testing Procedures," Available at http://ecfr.gpoaccess.gov/cgi/t/text/text-idx?c=ecfr&sid=024e8bd580a1b0936f51ab7cfb1615f1&rgn=div5&view=text&node=40:32.0.1.1.10&idno=40, Last Accessed: September 30, (2013).

32 "Light-Duty Vehicle Greenhouse Gas Emission Standards and Corporate Average Fuel Economy Standards; Final Rule," US Environmental Protection Agency, Federal Register Vol. 75, No. 88, May 7th, (2010).

33 Hadler, J., Rudolph, F., Dorenkamp, R., Kosters, M., Mannigel, D., and Veldten, B., "Volkswagen's New 2.0l TDI Engine for the Most Stringent Emission Standards - Part 2," MTZ Worldwide, Vol. 69, June, (2008).

34 Suresh, A., Khan, A., and Johnson, J.H., "An Experimental and Modeling Study of Cordierite Traps - Pressure Drop and Permeability of Clean and Particulate Loaded Traps," SAE Technical Paper No. 2000-01-0476, (2000).

35 Besch, M.C., Thiruvengadam, A., Kappanna, H.K., Cozzolini, A., Carder, D.K., Gautam, M., and Tikkanen, J., "Assessment of Novel In-Line Particulate Matter Sensor with Respect to OBD and Emissions Control Applications," Proc. of the ASME 2011 ICE Division Fall Technical Conference, Paper No. ICEF2011-60142, Morgantown, WV, Oct. 2nd-5th, (2011).

36 Andersson, J., Clarke, D., and Giechaskiel, B., "UN-GRPE Phase 3 Inter-Laboratory Correlation Exercise: Updated Framework and Laboratory Guide for Heavy-Duty Engine Testing." Working Paper No.GRPE-PMP-22-4, 22nd PMP working meeting, December (2007).

37 Giechaskiel, B., Ilara, P., and Andersson, J. "Particle Measurement Programme (PMP) light-duty inter-laboratory exercise: Repeatability and reproducibility of the particle number method," Aero. Sci. Technol., Vol. 42, Issue 7, pp. 528-543, (2008).

38 Andersson, J., Mamakos, A., Giechaskiel, B., Carriero, M., and Martini, G., "Particle Measurement Programme (PMP) Heavy-duty Inter-laboratory Correlation Exercise (ILCE_HD)," Final Report, Joint Research Center, Institute for Energy, EUR 24561 EN, (2010).

39 Johnson, K., Durbin, T.D., Jung, H., Chaudhary, A., Cocker III, D.R., Herner, J.D., Robertson, W.H., Huai, T., Ayala, A., and Kittelson, D., "Evaluation of the European PMP Methodologies during On-Road and Chassis Dynamometer Testing for DPF Equipped Heavy-Duty Diesel Vehicles," Aerosol Science and Technology, Vol. 43, pp. 962–969, (2009).

40 Zheng, Z., Johnson, K.C., Liu, Z., Durbin, T.D., Hu, S., Huai, T., Kittelson, D.B., and Jung, H.S., "Investigation of solid particle number measurement: Existence and nature of sub-23 nm particles under the PMP methodology," Journal of Aerosol Science, Vol. 42, pp. 883-897, (2011).

41 Jung, H., Zheng, Z., Durbin, T.D., and Johnson, K.C., "Issues associated with solid particle measurement," ARB Chairman's air pollution seminar series, January 24th, (2012).

42 Thiruvengadam, A., Besch, M.C., Carder, D.K., Oshinuga, A., and Gautam, M., "Influence of Real-World Engine Load Conditions on Nanoparticle Emissions from a DPF and SCR Equipped Heavy-Duty Diesel Engine," Environmental Science and Technology, Vol. 46, pp. 1907-1913, (2011).

43 Vaaraslathi, K., Keskinen, J., Giechaskiel, B., Solla, A., Murtonen, T., and Vesala, H., "Effect of Lubricant on the formation of Heavy-Duty Diesel Exhaust Nanoparticles," Environmental Science and Technology, Vol. 39, pp. 8497-8504, (2005).

44 Kittelson, D.B., Watts, W.F., Johnson, J.P., Thorne, C., Higham, C., Payne, M., Goodier, S., Warrens, C., Preston, H., Zink, U., Pickles, D., Goersamnn, C., Twigg, M.V., Walker, A.P., and Boddy, R., "Effect of fuel and lube oil sulfur on the performance of a diesel exhaust gas regenerating trap," Environmental Science and Technology, Vol. 42, pp. 9276-9282, (2008).